

8-2019

Fasting Reduces Intestinal Radiotoxicity Enabling Dose-Escalated Radiotherapy For Pancreatic Cancer

Marimar de la Cruz Bonilla

Follow this and additional works at: https://digitalcommons.library.tmc.edu/utgsbs_dissertations



Part of the [Cancer Biology Commons](#), and the [Radiation Medicine Commons](#)

Recommended Citation

de la Cruz Bonilla, Marimar, "Fasting Reduces Intestinal Radiotoxicity Enabling Dose-Escalated Radiotherapy For Pancreatic Cancer" (2019). *Dissertations and Theses (Open Access)*. 969.
https://digitalcommons.library.tmc.edu/utgsbs_dissertations/969

This Dissertation (PhD) is brought to you for free and open access by the MD Anderson UTHealth Houston Graduate School at DigitalCommons@TMC. It has been accepted for inclusion in Dissertations and Theses (Open Access) by an authorized administrator of DigitalCommons@TMC. For more information, please contact digcommons@library.tmc.edu.

FASTING REDUCES INTESTINAL RADIOTOXICITY ENABLING DOSE-
ESCALATED RADIOTHERAPY FOR PANCREATIC CANCER

by

Marimar de la Cruz Bonilla, BS

APPROVED:

Helen Piwnica-Worms, PhD
Advisory Professor

Cullen M. Taniguchi, MD/PhD

Michelle Barton, PhD

Russell Broaddus, MD/PhD

Anirban Maitra, MBBS

APPROVED:

Dean, The University of Texas
MD Anderson Cancer Center UTHHealth Graduate School of Biomedical
Sciences

FASTING REDUCES INTESTINAL RADIOTOXICITY ENABLING DOSE-
ESCALATED RADIOTHERAPY FOR PANCREATIC CANCER

A

DISSERTATION

Presented to the Faculty of

The University of Texas

MD Anderson Cancer Center UTHealth

Graduate School of Biomedical Sciences

in Partial Fulfillment

of the Requirements

for the Degree of

DOCTOR OF PHILOSOPHY

by

Marimar de la Cruz Bonilla, BS
Houston, Texas

August, 2019

Dedication

To my family, the one that raised me and the one I'm building; Jaime, Mami, Papi,
Gabriel, Vince, Mila and Maia you are my reason to exist.

Acknowledgements

Completing my PhD thesis project has required the support of a small army composed of mentors, colleagues, friends and family.

First and foremost, I'd like to thank both the Taniguchi and Piwnica-Worms' labs for always being there to teach me, help with experiments, edit my writing, and give feedback on oral presentations. Both my mentors; Helen Piwnica-Worms and Cullen Taniguchi were paramount in my growth as a scientist and taught me a deep love and respect for science that I will carry with me throughout my career. The postdoctoral fellows which I had the pleasure of training with; Dr. Gloria Echeverria, Dr. Kristina Stemler, Dr. Vidya Sinha, Dr. Emily Powell, and Dr. Abena Redwood taught me most of my technical skills and were key contributors to experimental design and data analysis throughout my five years of training. Additionally, Sabrina Jeter-Jones, Jessica Molkentine and Tara Fujimoto were vital collaborators in all animal experiments.

My friends were also key in maintaining my mental health intact throughout this process. To my friends in Puerto Rico and Houston, you've been my safe heaven throughout this process. I'd like to specially thank my friends who became sisters; Selena, Sarah, Neyda, Carolina, and Natalia; you have been there for all the crazy turns my life has taken these past five years and your support has been one of my main drivers for success.

Through the five years I have conducted the research presented here I had the pleasure of meeting two people who unfortunately were diagnosed with cancer. They have allowed me to be part of their war against this terrible disease. One of

them, Neggie, just recently lost her final battle to melanoma but thanks to her I was always cognizant of why we spend the extra time trying to understand how cancer works and novel ways to treat it. These interactions provided increased fuel, especially on days where science was not cooperating. I would like to thank her family for becoming a second family in Houston and sharing the highs and lows together.

Last, but certainly most important, I'd like to thank my family. You've supported me through my successes and failures always reminding me of what's important. To my parents, thank you for teaching me to be persistent, complete what I've started, and always do my work with love. To my brothers, my success is yours also, I wish that we continue being there for each other even when we're so incredibly different. To my husband, you are the main reason why I am writing this book. You've been my greatest cheerleader, my biggest fan, the most thorough editor, and most attentive audience. Because you are in my life, I decided to take a leap to complete my PhD and for that I will be eternally grateful. You have given me the greatest gift, confidence in myself and more room to dream big. I am very excited to see what science has in store for us, I'm sure by your side I can overcome any obstacle. Thank you for pushing me to be my best self.

There are many other people that have been a part of this journey be it personally or professionally. Thank you to my advisory committee, graduate school, MD/PhD program, and medical school. If I could go back I'd do it all over again, with all the same people to surround myself with, as this experience has been the most enriching of my life to date.

FASTING REDUCES INTESTINAL RADIOTOXICITY ENABLING DOSE-ESCALATED RADIOTHERAPY FOR PANCREATIC CANCER

Marimar de la Cruz Bonilla, BS

Advisory Professor: Helen Piwnica-Worms, PhD

Surgical resection is the only potentially curative treatment for pancreatic cancer, but only 15-20% of patients have resectable tumors. In unresectable cases, stereotactic body radiotherapy (SBRT) may be used to give tumor-directed radiotherapy (RT). Unfortunately, this can cause severe gastrointestinal (GI) toxicity due to proximity of the pancreatic head to the duodenum. Protecting the intestine from the toxic side-effects of radiation may enable dose-escalation that could achieve more effective local control of disease. We and others have previously shown that a fast of 24 hours protects mice from lethal doses of the DNA-damaging agent etoposide. In this study, we demonstrate that a 24 hour fast also protects mice from lethal doses of total-abdominal radiation. Histologic analyses using the Withers-Elkind microcolony assay show that fasting protected small intestinal (SI) stem cells from radiation damage and promoted early regeneration. To show a proof-of-principle for the use of this radioprotective maneuver in cancer therapy, we used an orthotopic model of pancreatic cancer using KPC tumor cells syngeneic to C57BL/6. Here, we show that fasting-mediated intestinal protection enabled dose escalated SBRT for treatment of these orthotopic tumors. RT with fasting-mediated radioprotection delayed tumor growth and improved survival compared to controls. Given this robust phenotype, we developed a 3D culture ex vivo assay using

intestinal stem cell-enriched epithelial spheroid cultures. We modified these intestinal spheroids with a bioluminescent reporter and used these cells to develop a modified clonogenic assay for 3D culture that can be used to identify novel radioprotectors, such as a fasting mimetic. Taken together, these results suggest that fasting protects small intestinal stem cells, allowing animals to receive potentially curative doses of abdominal radiation that would otherwise be lethal. Future work will aim to identifying the mechanisms by which fasting confers intestinal protection and drug candidates that can be used to mimic this fasting-mediated protection.

Table of Contents

TITLE PAGE	I
DEDICATION	II
ACKNOWLEDGEMENTS	III
ABSTRACT	V
TABLE OF CONTENTS	VIII
LIST OF ILLUSTRATIONS	X
LIST OF TABLES	XII
CHAPTER 1 – INTRODUCTION	1
FASTING IN STRESS-RESPONSE	2
FASTING AND CANCER THERAPIES	3
RADIATION INDUCED GASTROINTESTINAL SYNDROME	5
SMALL INTESTINAL EPITHELIUM DYNAMICS.....	6
INTESTINAL RADIOPROTECTORS.....	8
PANCREATIC CANCER	9
RADIATION THERAPY IN PANCREATIC CANCER.....	10
CHAPTER 2: METHODS AND MATERIALS	12
STUDY APPROVAL.....	13
MICE	13
KPC CELL GROWTH	13
ORTHOTOPIC INJECTIONS.....	13

ANIMAL ULTRASOUND	14
SMALL ANIMAL IRRADIATION	14
IMMUNOHISTOCHEMISTRY AND IMMUNOFLUORESCENCE	15
STATISTICAL ANALYSIS.....	17
REAGENTS, MEDIA AND DRUGS FOR SPHEROID FORMATION ASSAY	17
EQUIPMENT AND CONSUMABLES FOR SPHEROID FORMATION ASSAY	18
GENERATION OF SI STEM CELL ENRICHED SPHEROID CELL LINE	18
GENERATION OF SI STEM CELL ENRICHED SPHEROIDS EXPRESSING MCHERRY AND CBR- LUC	19
SPHEROID FORMATION ASSAY (SFA).....	20
BRIGHTFIELD SFA	20
BIOLUMINESCENT SFA.....	21
IMMUNOFLUORESCENT STAINING OF SPHEROIDS.....	22
CHAPTER 3: FASTING REDUCES INTESTINAL RADIOTOXICITY ENABLING DOSE-ESCALATED RADIOTHERAPY FOR PANCREATIC CANCER	23
ABSTRACT.....	24
INTRODUCTION	26
RESULTS.....	28
<i>Fasting protects wild-type mice from radiation-induced death</i>	<i>28</i>
<i>Fasting protects SI stem cells, enabling recovery of SI epithelium after radiation </i>	<i>31</i>
<i>Pre-radiation fasting does not reduce tumor response to radiation.....</i>	<i>46</i>
DISCUSSION	57

CHAPTER 4: STEM CELL ENRICHED-EPITHELIAL SPHEROID CULTURES FOR RAPIDLY ASSAYING SMALL INTESTINAL RADIOPROTECTORS AND RADIOSENSITIZERS <i>IN VITRO</i>	61
ABSTRACT.....	62
INTRODUCTION	63
RESULTS.....	66
<i>Development of the Spheroid Formation Assay (SFA)</i>	66
<i>SFA assay for identifying radioprotectors</i>	70
<i>Development of modified SFA that employs bioluminescence</i>	71
<i>Bioluminescent SFA to assay radioprotection</i>	73
<i>Application of Bioluminescent SFA for identifying radiosensitizers</i>	76
DISCUSSION	81
CHAPTER 5: DISCUSSION	82
BIBLIOGRAPHY	91
VITA	113

List of Illustrations

Figure 1 Optimization of total abdominal radiation (TA-XRT) maximum tolerated dose (MTD) for pre-radiation fasted mice.....	28
Figure 2 Illustration of sub-xyphoid 25-mm cone radiation field.....	29
Figure 3 Twenty-four hour fasting protects mice from radiation-induced death.	30
Figure 4 Fasting protects SI stem cells from high dose radiation.....	33
Figure 5 Fasting induced-protection of small intestinal stem cells allows for intestinal epithelium recovery after radiation.	37
Figure 6 Long term effects of high dose radiation.....	40
Figure 7 Effects of pre-radiation fasting on IR-induced DNA damage and apoptosis.....	43
Figure 8 Twenty-four hour fasting did not reduce the number of crypt epithelial cells staining positive for Ki67 relative to fed controls.....	45
Figure 9 Diagnostic ultrasounds of pancreatic tumor.....	46
Figure 10 Pre-radiation fasting does not confer protection to orthotopic KPC pancreatic tumors.....	49
Figure 11 Individual tumor growth curves.....	52
Figure 12 Pancreatic tumor viability in fed or fasted states following IR	53
Figure 13 Pre-radiation fasting does not confer protection to KPC tumors.....	56
Figure 14 Spheroid formation assay to identify GI radioprotectors.....	68
Figure 15 Generation of stem cell-enriched epithelial spheroid line stably expressing both Click Beetle Red Luciferase (CBR-Luc) and mCherry	72

Figure 16 Spheroid Formation Assay for identifying radioprotectors *in vitro*. 75

Figure 17 Spheroid Formation Assay for identifying radiosensitizers *in vitro*. 78

List of Tables

Table 1 Recorded cause of death in tumor-bearing mice 55

Chapter 1 – Introduction

This chapter is based upon (insert full citation)

Fasting in stress-response

A myriad of model organisms have been shown to withstand different stressors when they are subjected to an environment with decreased nutrition. In yeast and bacteria such as *E.coli*, starvation induces oxidative stress response genes leading to resistance to oxidative stress (1-3). In yeast, inducing starvation by growing cells in water not only induces protection against oxidative stress but also against heat shock(4). In worms, every two days of fasting protects from oxidative stress and increased lifespan (5, 6), whereas excessive glucose shortened lifespan (7).

Stress resistance in these organisms is promoted, at least in part, by downregulation of nutrient-signaling proteins, and consequent de-repression of stress resistance transcription factors (8). For example, yeast starvation-induced protection is thought to be as a consequence of reduced Ras/cAMP/PKA and Tor/S6K signaling and subsequent activation of factors downregulated by these pathways (4, 9-12). Similarly, in worms, fasting-induced protection occurs via alteration of the RHEB-1 and TOR pathways which are linked to DAF-16 (FOXO transcriptional factor homolog) (5, 6). Moreover, mutations in the PI3K homolog (*age-1*) and IGF-I receptor homolog (*daf-2*) in *C. elegans* decrease AKT-1/AKT-2 signaling and activates DAF-16, thereby extending lifespan and promoting stress resistance in these organisms (13-18). In flies, fasting increases d4E-BP expression which acts downstream of Pi3K/Akt/dFOXO3. Increased d4E-BP suppresses eIF4B-induced translation, moving energy away from growth and into protection from oxidative stress (19, 20).

In mice, the GH and IGF-I signaling axis controls stress resistance and lifespan. Transgenic mice overexpressing GH have decreased activity of superoxide dismutase

and catalase in their hepatocytes, indicating decreased oxidative stress response (21, 22). The opposite is also observed as cells derived from mice with GH/IGF-I deficiencies are resistant to a myriad of stressors including UV, genotoxins, heat and oxidative stress (23, 24). IGF-I has also been shown to sensitize neurons, primary glia and fibroblasts to oxidative damage and genotoxic drugs (25, 26).

Fasting and Cancer Therapies

Caloric restriction, a reduction of the daily consumed calories by 10-50%, has been shown to delay the progression of some tumors and to prevent the growth of transplanted tumors in mice (27, 28). In fact, caloric restriction has been shown to increase lifespan and decrease cancer incidence in mice, rats and primates (29-31). The effect of caloric restriction on tumor growth varies. On the one hand, tumors with loss of PTEN function or PI3K activating mutations have been shown to be resistant to dietary restriction (32). Tumors that are sensitive to dietary restriction experience a decrease in Akt signaling that accompanies the decrease in available circulating growth factors, whereas tumors with constitutive PI3K signaling activation, and thus downstream auto-growth signals, are not affected by environmental shifts in nutrient availability (32). In this context, sensitive tumors were found to increase pro-apoptotic and anti-proliferative gene expression mediated by FOXO1 transcription factor relocalization to the nucleus (32). This observation denotes the importance in understanding the metabolic drivers of tumor development and growth to better identify cases in which dietary interventions such as caloric restriction or fasting could be applied.

Fasting, on its own suppresses tumor growth in mice. It has been shown to decrease the incidence of lymphomas (33) and delay spontaneous tumor formation in p53-deficient mice (34). The greatest therapeutic response is found when fasting is combined with chemotherapy when compared to either intervention alone (35). On the other hand, it has not yet been determined whether tumors that are resistant to dietary restriction are more or less sensitive to chemotherapy (32).

The study of clinical applications of fasting in cancer therapy is still very limited. Cancer patients undergoing chemotherapy experience high rates of morbidity, despite regimens that attempt to balance timing and dose intensity to mitigate off-target effects and dose limiting toxicities (36). In addition, life-threatening side effects experienced by cancer patients undergoing treatment limit the feasibility of dose-escalation regimens to kill their tumors. Although caloric restriction has not been as successful in inducing protection (37) of normal cells, fasting has been shown to protect the host, but not engrafted tumors from the toxicity associated with high-dose chemotherapy (35, 38). Long-term fasting has been used to mitigate toxicity from etoposide, doxorubicin, cyclophosphamide, and 5-Fluorouracil in mice (26, 38) and further from docetaxel, carboplatin, paclitaxel, and gemcitabine in a patient case series (39, 40). Specifically, patients who fasted prior to receiving chemotherapy reported fewer side effects (including reduced GI side effects) and with no evidence that fasting protected tumors or interfered with chemotherapy efficacy (39). Thus, fasting can reduce side effects associated with chemotherapy without negatively impacting tumor cell killing. Unfortunately, fasting is not feasible for all cancer patients, especially those exhibiting cachexia. A mechanistic understanding of how fasting protects SI stem cells may

identify ways to protect patients from the deleterious side effects of cancer therapies without the need for them to fast. Previous work from our lab provides mechanistic insight into how fasting provides host protection from high-dose etoposide. Previously, we demonstrated that short-term fasting protects small intestinal stem cells from lethal doses of DNA damage and this, in turn, preserves SI homeostasis and promotes organismal survival. DNA repair and DNA damage response genes were elevated in SI stem cells of fasted etoposide-treated mice, which importantly correlated with faster resolution of DNA DSBs and less apoptosis.

Approximately half of cancer patients receive some sort of radiation during their treatment. Radiation is not a targeted therapy; it causes negative effects on normal tissues that are in the radiation field. The bone marrow and the small intestine are the first and second most radiosensitive organs, respectively (41). As such, patients undergoing radiation for abdominopelvic malignancies or whole-body radiation for bone marrow transplant are at risk of suffering from gastrointestinal side effects due to radiation toxicity. The work presented here demonstrates that fasting also provides host protection from high-dose ionizing radiation.

Radiation Induced Gastrointestinal Syndrome

Radiation-induced gastrointestinal syndrome (RIGS) occurs when patients are exposed to high doses (>10 Gy) of radiation. Radiation targets the fast cycling stem cells in the intestinal crypts. Continued migration of differentiated epithelial cells from crypts to villi and ultimately sloughing into lumen, without a stem cell reservoir to

replenish villi, will result in denuding of the intestinal epithelium with stunted villi and decreased absorptive surface area (42-44). Clinically, acute symptoms of RIGS include abdominal pain, bloating, appetite loss, nausea and diarrhea (45). Chronically, patients can develop post-prandial pain, small bowel obstruction, nausea, anorexia, malabsorption or diarrhea (46). As such, patients may present with significant morbidities including dehydration, electrolyte imbalance, weight loss and exhaustion. Additionally, sufficient crypt loss can lead to breakage of the intestinal barrier allowing gut flora to access the bloodstream which can cause sepsis and subsequent death (41). Depending on severity and decline of the patients' quality of life associated to RIGS, up to 20% of patients have had to alter their therapy due to GI radiation toxicities (47).

Although immediately after radiation, p53 induces PUMA mediated apoptosis in the SI (48-50), it also allows for a p53/p-21 cell cycle arrest in small intestinal cells (51) which may play a role in the prevention of mitotic catastrophe and subsequent stem cell death. In fact, mice deficient in p53 were observed to bypass the p21 checkpoint allowing crypt cells to continue cycling. This lead to accelerated death of damaged cells and decreased survival (51). Interestingly, fasting has been shown to increase the expression of p21 in mouse tissues, including in the small intestine (52), yet the potential role of p21 expression in fasting-mediated small intestinal chemoprotection has not been studied.

Small Intestinal Epithelium Dynamics

The small intestinal epithelium is composed of villi and crypts. There are four differentiated cell types: absorptive (enterocytes), goblet, endocrine and paneth cells (53). The first three reside in the villi where enterocytes absorb nutrients, goblet cells secrete mucus and enteroendocrine cells release hormones. Paneth cells reside in the crypt and form part of the small intestinal stem cell niche. SI crypts compose the proliferative compartment of the small intestine from which stem cells produce rapid cycling transit amplifying (TA) cells, which continue differentiating and migrating upwards through the villi and are ultimately sloughed off into the intestinal lumen resulting in an intestinal epithelium turnover of 4-5 days (54).

Two types of stem cells have been identified in the mouse small intestine: the crypt base columnar (CBC) cells, which are interspersed with Paneth cells at the bottom of the crypt and the +4 cells (55, 56). CBCs are multipotent stem cells marked by the expression of LGR5 and are highly proliferative cycling every 24h (57, 58). Several putative +4 stem cell markers have been shown to lead to lineage tracing in vivo. Bmi1 was described to mark cells at the +4 position which were self-renewing multipotent stem cells (59). Unfortunately, the specificity of Bmi1 as a +4 stem cell marker has been challenged since studies have found Bmi1 being expressed in Lgr5+ stem cells and Bmi1 has been observed in cells spanning varied positions around the crypt (CITE DOI 10.1073/pnas.1013004108 (60, 61). HopX, Lrig1, and Tert have independently been shown to be markers of quiescent stem cells, residing around the +4 position, which can generate labeled progeny (62-64). However, the expression of these marks does not appear to be specific to one stem cell population which confounds the SI stem cell model. Due to this, a newer model has been proposed

where both groups of stem cells, the CBC and the +4, coexist for different physiological roles. The CBC cells are afforded the function of maintaining intestinal homeostasis during normal turnover of the epithelium and the +4 cells are thought to function as a reserve stem cell pool that is activated in the setting of intestinal injury (65).

Intestinal Radioprotectors

Despite the fact that toxicity to the GI tract is a significant clinical problem, there are no existing approved normal tissue protectors that can prevent this toxicity. Amifostine is the only FDA approved radiation protector, but its use is limited by severe side effects such as hypotension and nausea (66). Thus, identification of novel radioprotectors could not only improve patients' quality of life by reducing the aforementioned side effects, but also increase the therapeutic window to enable dose escalation of cytotoxic therapy and more effective tumor cell killing.

The classical assay to assess the cellular radiation response is the clonogenic assay, or colony formation assay, which monitors the ability of a single tissue culture cell to grow into a colony after administration of radiation or chemotherapy(67). Unfortunately, the discovery of novel protective drugs by this assay is limited by the technical difficulties of culturing normal tissues *ex vivo*. Cell lines such as Caco-2 (colon cancer derived cells) or Hs 1.Int (non-epithelial intestinal derived cells) have been used to approximate intestinal function, but are often inadequate for estimating the ability to respond to radiation since neither of them are truly representative of normal cells (68).

The gold standard for studying the response of the intestinal tract to cytotoxic insult is the microcolony assay developed by Withers and Elkind (69), which assesses regenerating intestinal stem cells after cytotoxic therapy. This method utilizes a single lethal or sublethal administration of cytotoxic therapy (e.g. radiation) that kills existing intestinal stem cells in the crypt. Nascent stem cells that regenerate after the cytotoxic insult are identified by a histopathological technique that requires transverse sections of intestine on a single slide, which can be technically demanding(69). Even if the slides are prepared properly, the individual regenerating crypts must be counted manually by an experienced pathologist. Lastly, implicit in this assay is that each data point requires large numbers of mice, making the entire process both costly and low throughput for identifying and characterizing new modulators of intestinal damage.

The advent of intestinal stem cell enriched-spheroids grown from murine or human tissue *ex vivo* has enabled the study of normal intestinal tissue and its responses to radiation (70) or chemotherapy (71). These cultures, which are amenable to genetic modification(72), can be passaged indefinitely using growth factor-enriched media in a 3D matrix. Here, we describe the development of a modified colony formation assay, which we refer to as a spheroid formation assay (SFA), that establishes a small intestinal (SI) stem cell-enriched spheroid cell line directly from mice to study the effects of radiation or chemotherapy treatments *ex vivo*.

Pancreatic Cancer

Pancreatic ductal adenocarcinoma (PDAC) is expected to become the most common cause of cancer-related deaths by 2030(73). There has been little

improvement in PDAC prognosis over the last several decades, and the 5-year survival rate of pancreatic cancer remains below 10%(74). Currently, the most effective treatment for PDAC is surgery. However, because of the late onset of symptoms, only 15-20% of patients present with resectable disease, whereas the remaining 80%–85% present with locally advanced unresectable or metastatic disease. Chemotherapy combined with radiotherapy (RT) is the most commonly used approach for treating locally advanced unresectable pancreatic cancer.

Radiation therapy in pancreatic cancer

The amount of chemotherapy and radiation that can be given to cancer patients is limited due to the sensitivity of normal tissues. This issue is highlighted with radiation therapy, which can kill solid tumors anywhere in the body but also damages adjacent normal tissue. For instance, cancers of the abdomen and pelvis, such as pancreatic and prostate adenocarcinoma, are difficult to ablate with radiation alone because these tumors require high doses of radiation for control, but are often adjacent to very radiosensitive structures of the GI tract, such as the small intestine(75). This is perhaps best illustrated by locally advanced cancer of the pancreatic head since potentially curative doses of radiation (60-70Gy) are constrained by the nearby duodenum, which can only tolerate a maximum of 50Gy (76). This potential for morbid toxicity, often prevents these tumors from receiving a definitive therapeutic dose. In addition, chemotherapeutic agents, such as irinotecan and anti-angiogenic biologics such as bevacizumab, also have dose limiting GI toxicities, including potentially fatal diarrhea and bowel perforation(77, 78).

Results from phase I/II trials have demonstrated that dose escalation is possible with sophisticated radiation techniques like intensity-modulated radiation therapy (IMRT)(79). Though these conformal techniques are highly precise, they often cannot avoid the duodenum which abuts the pancreas. Moreover, considerable expertise is required for dose-escalated radiation within the abdomen or pelvis, which limits these treatments to a handful of academic centers. Thus, a complementary and potentially more tractable method to improve the therapeutic ratio for chemoradiation for tumors within the abdomen or pelvis may be to reduce toxicity to the GI tract with a radioprotectant. Moreover, by reducing side effects from radiation damage, a radioprotectant drug could increase the quality of life for our cancer survivors. Here we test the hypothesis that by protecting the small intestine from high-dose radiation, fasting allows dose escalation for efficient killing of pancreatic tumor cells in a murine model of PDAC (80).

Chapter 2: Methods and Materials

Study Approval. This study was carried out in accordance with the recommendations in the Guide for the Care and Use of Laboratory Animals from the National Institutes of Health (NIH) Institutional Animal Care and Use Committee (IACUC). The protocol was approved by the IACUC at MD Anderson Cancer Center (Protocol #1101RN01). Animals were euthanized as dictated by the Association for Assessment and Accreditation of Laboratory Animal Care International and IACUC euthanasia endpoints.

Mice. Both male and female mice were used in this study. C57Bl/6J mice (stock no. 000664) were purchased from The Jackson Laboratory. Nine-week-old male mice used for survival and intestinal histology experiments weighed from 23.4g to 26.6g, whereas female mice ranged from 18.1g to 20.5g.

KPC Cell Growth. The KPC cell line was derived from a spontaneous tumor from a female *KrasG12D^{LSL/+}; Trp53 R172H; Pdx1-Cre* (KPC) mouse(81). KPC cells were maintained in RPMI 1640 (Sigma Aldrich) supplemented with 1% GlutaMAX™, 1% sodium pyruvate, and recombinant insulin (all from Life Technologies). Media was supplemented with 10% regular fetal bovine serum (Heat-inactivated, Atlanta Biologicals).

Orthotopic Injections. KPC cells were resuspended in RPMI 1640 (Sigma Aldrich) and mixed with chilled Matrigel in a 1:1 ratio. Mice were anesthetized with 2% isoflurane and supported with artificial eye drops and a prophylactic dose of 0.1 mg/kg

extended release buprenorphine given subcutaneously for post-operative analgesia. Mice were placed in the right lateral decubitus position, fur was shaved and wiped with a 10% povidone iodine solution and 70% ethanol. Through a 1.5 cm incision with sterile surgical instruments, the spleen was visualized and removed from the abdominal cavity exposing the underlying tail of the pancreas. KPC cells (2×10^4 cells) in 20 μ L of Matrigel were injected into the pancreatic parenchyma and observed until the Matrigel solidified. The organs were returned and the abdomen was closed with absorbable 6-0 sutures and surgical staples. Mice were observed as they recovered from their operation. Tumors were allowed to grow for two weeks and then monitored with ultrasound imaging.

Animal Ultrasound. Mice were subjected to 2% isoflurane for anesthesia, and treated with epilation cream. Animals were then placed onto a Vevo 2100 system (FujiFilm VisualSonics). A 30 MHz transducer was used to acquire B-MODE long and short axis acquisitions(81). Tumor measurements were made every 4-5 days until animal death or euthanasia.

Small Animal Irradiation. Small animal irradiation was performed as previously described(82). Experimental mice were singly housed on aspen bedding. Mice were allowed to feed *ad libitum* or were fasted for 24 h, followed by total abdominal radiation (TA-XRT). Mice were treated on an X-RAD 225Cx machine with an isoflurane anesthesia manifold and on-board image guidance. Beam arrangement was anterior-posterior/posterior-anterior using a 25-mm cone positioned under the

xyphoid process through image guidance by cone beam computed tomography. The final dose of TA-XRT was 11.5 Gy for C57Bl/6J non-tumor bearing mice and 12 Gy TA-XRT for tumor bearing mice. After treatment moistened food pellets were placed at the bottom of all cages.

Immunohistochemistry and Immunofluorescence. Mouse SI were harvested as described previously(71), and jejunum sections were used for all analyses. Microlony assays were performed using the classical Withers and Elkind technique(69). Briefly, jejunums were resected, fixed in 10% neutral buffered formalin, paraffin embedded, and cut transversely for subsequent H & E staining and analysis.

Immunofluorescence (IF) staining of tumor tissues for cleaved-caspase 3 (CC3) and γ -H2AX and of SI for Ki67, utilized triology (Cell Marque) for deparafinization, rehydration, and antigen retrieval according to the manufacturer's protocol (Fig. 4, S5 and S8). Sections were blocked using protein block (Dako). Following blocking, sections were incubated at 4°C overnight with primary antibody diluted in antibody diluent (Dako). Primary antibody concentrations were as follows: anti-phospho-Histone H2AX 1:250 (9718, Cell Signaling), anti-CC3 1:300 (9661, Cell Signaling), and anti-Ki67 1:1000 (ab15580, Abcam). Sections were washed and then incubated with secondary antibody for 30 min at room temperature in the same antibody diluent (Dako). Secondary antibodies included Alexa-Fluor 488 donkey anti-rabbit 1:500 (A-21206, ThermoFisher) for tumor staining and Alexa-Fluor 594 (A-11012, ThermoFisher) for SI staining. Sections for IF staining were washed with PBS, counter-stained with DAPI (1 μ g/mL) in PBS, washed, and coverslip-mounted using

fluorescent mounting media (Dako). Fluorescent images were acquired using a Nikon Eclipse Ni-E microscope, with Nikon Plan Fluor 40x/1.30 objective for tumor tissues and 20x/0.75 objective for SI, Andos Zyla sCMOS camera, and NISElements Advanced Research software.

Multiplexed staining of SI tissue for CC3 and γ -H2AX (Fig. 3) was performed using the Opal protocol as described previously(83). Slides were deparaffinized in xylene and rehydrated in ethanol. Slides were placed in a 1:10 dilution of ARF buffer in deionized water (Perkin Elmer) and antigen retrieval was performed in an Antigen EZ-Retriever v. 3.0 microwave oven. Sections were blocked using protein block (Dako) and then incubated at 4°C overnight in a 1:1000 dilution of anti-phospho-histone H2A.X (γ -H2AX) antibody (9718, Cell Signaling). Protein detection was performed using the ImmPRESS® HRP Anti-Rabbit IgG (Peroxidase) Polymer Detection Kit (Vector Laboratories) followed by incubation in a 1:100 dilution of Opal 570 (FP1488001KT, Perkin Elmer). Antigen retrieval and blocking steps were repeated and slides were incubated at 4°C overnight in a 1:1000 dilution of anti-CC3 antibody (9661, Cell Signaling). The secondary antibody was the same as used for (γ -H2AX) followed by incubation in a 1:100 dilution of Opal 520 (FP1487001KT, Perkin Elmer). Tissues were washed with PBS, counter-stained with DAPI (1 μ g/mL) in PBS, washed, and coverslip-mounted using fluorescent mounting media (Dako). Fluorescent images were acquired using a Nikon Eclipse Ni-E microscope, with Nikon Plan Fluor 20x/0.75 objective, Andos Zyla sCMOS camera, and NISElements Advanced Research software. Only those epithelial cells directly aligning the crypt were quantitated.

Statistical Analysis. The statistical analyses used in this study are described in each figure legend. Log-Rank analysis was used for survival studies and median survival was determined with 95% confidence interval (CI). Two tailed t-tests with unequal variance were used to compare the number of regenerating crypts per circumference of SI and for quantitating the immunofluorescence staining of SI. Tukey's multiple comparison test with a single pooled variance of a one-way ANOVA was used to compare crypt depth, crypts per mm, villi height, traced crypts, and for quantitating the immunofluorescence staining of tumor tissue. Values less than 0.05 were considered significant.

Reagents, media and drugs for Spheroid Formation Assay. Polybrene (Sigma-Aldrich), 1X Dulbecco's calcium and magnesium free phosphate buffered saline (DPBS) (Corning); Corning® Matrigel®™ Basement Membrane Matrix (Corning), Corning® Cell Recovery Solution CS100 ml (Corning); TrypLE™ Express Enzyme (1X), phenol red (Gibco); DMEM/F12 (Sigma Chemical Co.); ADMEM/F12 (Sigma Chemical Co.); HBSS (Ca²⁺-and Mg²⁺-free; Life Technologies); Fetal Bovine Serum – Premium Select (Atlanta Biologicals); L-Glutamine, 200 mM (Sigma-Aldrich); Penicillin, 10,000 Units/ml and streptomycin, 10,000 ug/ml (Hyclone); ViaStain™ AO/PI Staining Solution (Nexcelom); Corning® Matrigel® Basement Membrane Matrix, *LDEV-Free, 10 mL (Corning); L-WRN cell 50% conditioned media (prepared as described in(72)); ROCK Inhibitor (Y-27632) (Sigma-Aldrich); TGF-β RI Kinase Inhibitor VI (SB431542) (EMDMillipore); D-Luciferin, Potassium Salt (Proven and

Published™) (Gold Biotechnology); N-acetylcysteine amide (NAC), (Sigma Aldrich); WR-1065 (Sigma-Aldrich), SN-38 (Selleck Chemicals); and Dimethyl sulfoxide, Hybri-Max™, sterile-filtered, BioReagent (Sigma-Aldrich).

Equipment and consumables for Spheroid Formation Assay. The following equipment and consumables were used to develop the SFA: Cellometer® Vision Cell Profiler CBA (Automated Cell Counter); CLARIOstar (BMG Labtech); Cytation 3 (Biotek); Clear cell culture plate, 24 well (Thermo-Fisher); Black wall clear bottom cell culture assay plate, 24 well (MIDSCI); 5 ml Falcon® round bottom tubes with cell strainer cap (Corning); Cellometer® Disposable Counting Chambers (Nexcelcom); X-RAD 320 Biological Irradiator (Precision X-Ray), VX-2500 Multi-Tube Vortexer (VWR)

Generation of SI stem cell enriched spheroid cell line. Crypt isolation and establishment of spheroid cultures were performed as described by Miyoshi et al. (2013)(72). For all steps in this procedure, DPBS and HBSS without calcium and magnesium were prepared and EDTA was added to a final concentration of 2 mM. All solutions were prepared before initiating harvest and placed on ice. Mice were euthanized and their entire small intestinal (SI) tract was isolated and flushed with DPBS. The SI were cut longitudinally and placed on ice in DPBS for 10 min, then transferred to ice-cold HBSS. Sections were vortexed at 1,600 rpm in HBSS for 5 min, changed to fresh HBSS, vortexed at 1,600 rpm for 3 min, then again placed into HBSS before vortexing at 1,600 rpm for 8 min. The cells were then changed to fresh HBSS and vortexed at 1,600 rpm for 5 min. All vortexing was conducted at 4°C.

Supernatants from the third and fourth vortexes were combined and passed through 80- μ m strainers (Corning) to isolate crypts and remove any villi that might remain in the washes. Crypts were pelleted at 100 \times g at 4°C, then resuspended in ADMEM/F12 supplemented with 10% (vol/vol) FBS, 10 U/mL penicillin, 10 μ g/mL streptomycin, and 2 mM L-glutamine, centrifuged at 400 \times g at 4 °C and resuspended in Matrigel. Crypts were plated in a 24-well tissue culture dish (30 μ l per well). After Matrigel solidification at 37°C, 50% (vol/vol) L-WRN conditioned media was supplemented with 10 μ M Y27632 (ROCK inhibitor) and 10 μ M SB431542 (TGF- β RI Kinase Inhibitor VI) and added to each culture well. Media was changed every second day and spheroids were passaged every third day.

Generation of SI stem cell enriched spheroids expressing mCherry and CBR-Luc. Lentiviral transduction of SI stem cell enriched spheroids was carried out as described(72). Briefly, cells were transduced with lentivirus encoding Click Beetle Red Luciferase (CBR-luc) and mCherry (FUW-CBR-luc-mCherry)(84) in the presence of 1 μ g/ml Polybrene for 6 h.

Cells were expanded for 7 passages, harvested using Cell Recovery Solution, digested to a single cell suspension using TrypLE supplemented with 10 μ M Y27632 and 500 μ M NAC and mCherry positive cells were isolated using an Influx cell sorter (BD Biosciences). Gating strategy included sorting on first forward/side scatter, then on singlets, and lastly mCherry positive expression. Sytox blue was used to exclude dead cells. Non-transduced cells from Passage 7 parental spheroid cultures served as a negative control for gating in the mCherry channel(84).

Spheroid Formation Assay (SFA). Spheroid cultures were placed in Cell Recovery Solution for 30 min on ice. Samples were transferred to a conical tube, centrifuged at 233 x g for 5 min at 4°C, washed with DPBS, centrifuged at 233 x g for 5 min at 4°C, trypsinized using TrypLE supplemented with 10 µM Y27632 and 500 µM NAC for 5 min at 37°C on a bead bath. Samples were pipetted up and down for 10 s once every minute for 5 min. TrypLE was neutralized with ADMEM/F12 supplemented with 10% (vol/vol) FBS, 10 U/mL penicillin, 10 µg/mL streptomycin, 2 mM L-glutamine, 10 µM Y27632 and 10 µM SB431542. Samples were centrifuged at 233 x g for 5 min at 4°C, resuspended in ADMEM/F12 supplemented as described above, and placed in a 5 ml Falcon® round bottom tube with 35 µM cell strainer cap to isolate single cells. Live cells were quantified using ViaStain™ AO/PI Staining Solution in the Cellometer® Vision CBA Image Cytometer. Five thousand live cells suspended in 30 µl of Matrigel were then placed in each well of five 24-well culture plates. After solidification of Matrigel at 37°C, 500 µl of 50% (vol/vol) L-WRN conditioned media containing 10 µM Y27632 and 10 µM SB431542 was added to each well. Media was changed every three days. When spheroids formed (3-8 days), cultures were exposed to the indicated pre-radiation treatment and then irradiated using the X-Rad 320.

Brightfield SFA. Cells were harvested and passaged as described above, incubated on ice with Cell Recovery Solution for 30 min and transferred to 15 mL conical tubes. They were then centrifuged at 233 x g for five minutes at 4°C and digested to single cells using supplemented TrypLE. Live cells were quantified and

5,000 live cells were plated in 30 μ L of Matrigel per well. Each sample was plated in triplicate on black wall clear bottom cell culture plates. Once Matrigel solidified, samples were supplemented with 50% (vol/vol) L-WRN conditioned media and spheroids were allowed to grow for 5 days. Conditioned media was changed every 3 days. Using a Cytation 3 Cell Imaging Multi-Mode Reader, spheroids were visualized using Z-stack images spanning 1.5 mm in height and covering the entire Matrigel dome area. The imaging protocol acquired 16-25 slices spanning 1500 μ m sample depth beginning at the bottom of the culture well and proceeding to the top of the Matrigel dome. Slices were merged to produce a single Z-stack image spanning the entire depth of the Matrigel dome. Twenty-one Z-stacked images were then manually stitched together using Adobe® Photoshop® to generate an image of the entire spheroid culture. Spheres measuring at least 150 μ m were manually quantified and surviving fraction was calculated as described previously(67).

Bioluminescent SFA. Immediately following brightfield image acquisition, D-Luciferin was dissolved in 50% conditioned media supplemented with 10 μ M Y27632 and 10 μ M SB431542 to a final concentration of 300 μ g/mL. Conditioned media was aspirated from each well and replaced with 500 μ l of D-Luciferin-containing conditioned media. Cultures were placed in the incubator for 10 to 30 min at 37°C. Bioluminescence was measured from the entire well using a CLARIOstar plate reader using top optic with a focal height of 5 mm at 1 second per well with no emission filter.

Immunofluorescent staining of spheroids. Spheroid cultures were washed with PBS and fixed with 4% paraformaldehyde for 1 h. Cells were collected and resuspended in Histogel™. Tissues were sectioned at a thickness of 5 µm. Trilogy (CellMarque) was used for deparafinization, rehydration, and antigen retrieval according to the manufacturer's protocol. Sections were blocked using protein block (Dako). Following blocking, sections were incubated at 4°C overnight with primary antibody diluted in antibody diluent (Dako). Primary antibody concentrations were as follows: antiphospho-Histone H2AX 1:250 (Cell Signaling, 9718), and anticlaved caspase 3 1:300 (Cell Signaling, 9661). Sections were washed and then incubated with secondary antibody for 30 min at room temperature in the same antibody diluent (Dako). Secondary antibody used was Alexa-Fluor 488 donkey anti-rabbit 1:500 (ThermoFisher, A-21206). Sections for immunofluorescence were washed with PBS, counterstained with DAPI (1 µg/mL) in PBS, washed, and coverslip-mounted using fluorescent mounting media (Dako). Fluorescent images were acquired using a Nikon Eclipse Ni-E microscope, with Nikon Plan Fluor 40×/1.30 objective, Andos Zyla sCMOS camera, and NISElements Advanced Research software.

Chapter 3: Fasting reduces intestinal radiotoxicity enabling dose-escalated radiotherapy for pancreatic cancer

This chapter is based upon “de la Cruz Bonilla, M., Stemler, K. M., Jeter-Jones, S., Fujimoto, T. N., Molkentine, J., Asencio Torres, G. M., Zhang, X., Broaddus, R.R., Taniguchi, C.M., Piwnica-Worms, H. (2019). Fasting Reduces Intestinal Radiotoxicity, Enabling Dose-Escalated Radiation Therapy for Pancreatic Cancer. *International Journal of Radiation Oncology • Biology • Physics*. <https://doi.org/10.1016/j.ijrobp.2019.06.2533>”

Abstract

Purpose

Chemotherapy combined with radiotherapy is the most commonly used approach for treating locally advanced pancreatic cancer. The use of curative doses of radiation in this disease setting is constrained due to the close proximity of the head of the pancreas to the duodenum. The purpose of this study was to determine if fasting protects the duodenum from high-dose radiation, thereby enabling dose escalation for efficient killing of pancreatic tumor cells.

Methods and Materials

C57BL/6J mice were either fed or fasted for 24 h and then exposed to total abdominal radiation at 11.5 Gy. Food intake, body weight, overall health and survival were monitored. Small intestines were harvested at various timepoints after radiation and villi length, crypt depth, and number of crypts per mm of intestine were determined. Immunohistochemistry was performed to assess apoptosis and double strand DNA breaks and microcolony assays were performed to determine intestinal stem cell regeneration capacity. A syngeneic KPC model of pancreatic cancer was employed to determine the effects of fasting on the radiation responses of both pancreatic cancer and host intestinal tissues.

Results

We demonstrated that a 24 h fast in mice improved intestinal stem cell regeneration by microcolony assay and improved host survival from lethal doses of total abdominal radiation when compared to fed controls. Fasting also improved survival of mice with orthotopic pancreatic tumors subjected to lethal abdominal radiation when compared

to controls with free access to food. Furthermore, fasting did not impact tumor cell killing by radiation therapy and enhanced γ -H2AX staining after radiotherapy, suggesting an additional mild radiosensitizing effect.

Conclusions

These results establish proof-of-concept for fasting as a dose-escalation strategy, enabling ablative radiation in the treatment of unresectable pancreatic cancer.

Introduction

Pancreatic ductal adenocarcinoma (PDAC) is expected to become the most common cause of cancer-related deaths by 2030(73). There has been little improvement in PDAC prognosis over the last several decades, and the 5-year survival rate of pancreatic cancer remains below 10%(74). Currently, the most effective treatment for PDAC is surgery. However, because of the late onset of symptoms, only 15-20% of patients present with resectable disease, and the remaining 80%–85% are incurable without appropriate local therapy. Chemotherapy combined with radiotherapy (RT) is the most commonly used approach for treating unresectable pancreatic cancer.

Unfortunately, radiation therapy cannot yet achieve curative doses for pancreatic cancer due to the sensitivity of the nearby gastrointestinal (GI) tract to radiation damage. Results from phase I/II trials have demonstrated that dose escalation is possible with sophisticated radiation techniques like intensity-modulated radiation therapy (IMRT)(79). Though these conformal techniques are highly precise, they often cannot avoid the duodenum which abuts the pancreas. Moreover, considerable expertise is required for dose-escalated radiation within the abdomen or pelvis, which limits these treatments to a handful of academic centers. Thus, a complementary and potentially more tractable method to improve the therapeutic ratio for chemoradiation for tumors within the abdomen or pelvis may be to reduce toxicity to the GI tract with a radioprotectant.

Interestingly, fasting has been shown to provide host-protective effects from the toxicity associated with high-dose chemotherapy in mice(26, 71) and in a patient case series(39). Importantly, fasting protects small intestinal (SI) stem cells thereby preserving SI homeostasis and promoting organismal survival in the presence of lethal doses of etoposide(71).

In the context of radiation, one study explored the use of prolonged fasting in combination with RT on a subcutaneous mouse model of glioma and reported sensitization of the tumor to radiation(85). Although the effects of caloric restriction and ketogenic diets on radiation response have been described(86), ours is the first study to examine the effects of short-term fasting on the radiation response of normal tissues. Here, we demonstrate that fasting protects mice from what would otherwise be a lethal dose of RT and we translate our findings to an aggressive mouse model of pancreatic cancer.

TA-XRT was performed using a circular 25 mm field to the abdomen placed below the xiphoid process (Fig. 2) to ensure radiation of the entire intestinal tract while sparing nearly all the bone marrow in the pelvis, thereby avoiding competing hematopoietic toxicity.

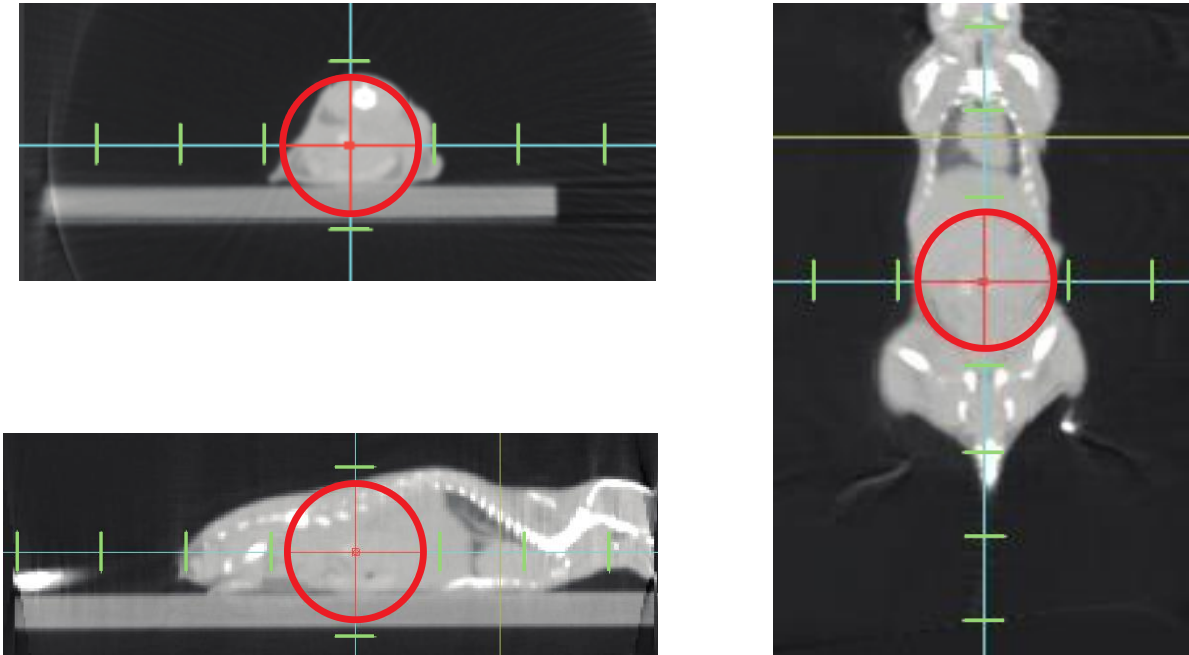


Figure 2 Illustration of sub-xyphoid 25-mm cone radiation field.

Illustration of sub-xyphoid 25-mm cone radiation field. Red circle denotes radiated area. Ticks are 12.5 mm from each other.

After radiation, mice were returned to their cages with free access to food and water and were monitored for 30 days, during which time food intake and body weight were recorded (Fig. 3A).

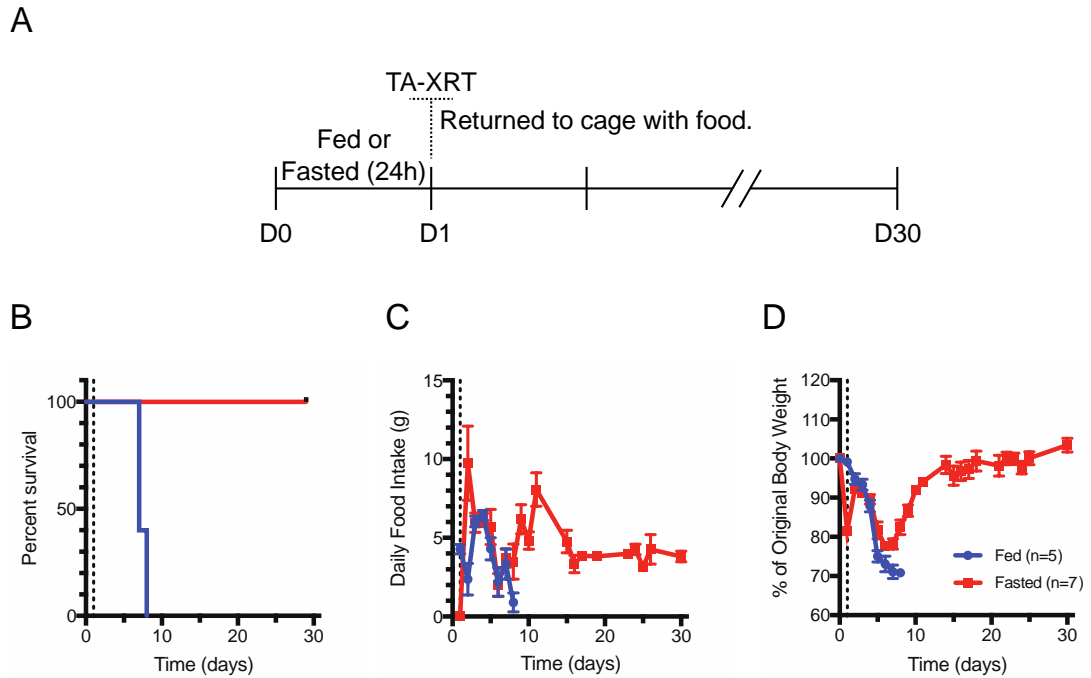


Figure 3 Twenty-four hour fasting protects mice from radiation-induced death.

(A) C57Bl/6J mice were allowed to feed *ad libitum* or were fasted for 24 h. Total abdominal radiation (TA-XRT; 11.5 Gy) was administered (day 1). Mice were returned to single-housed cages with food. (B) Survival was monitored daily. (C) Daily food intake and (D) individual mouse body weights were measured. All error bars are \pm SEM.

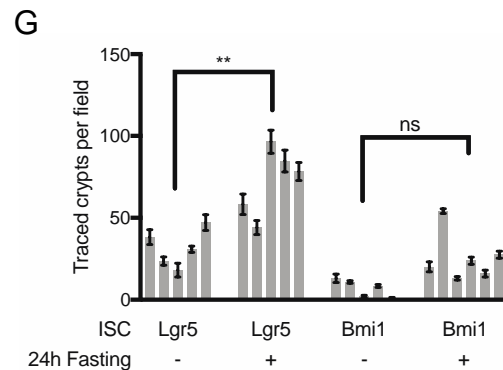
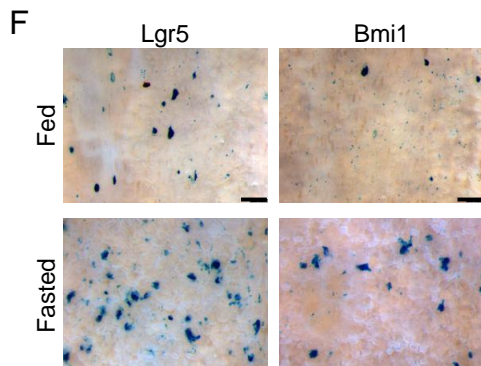
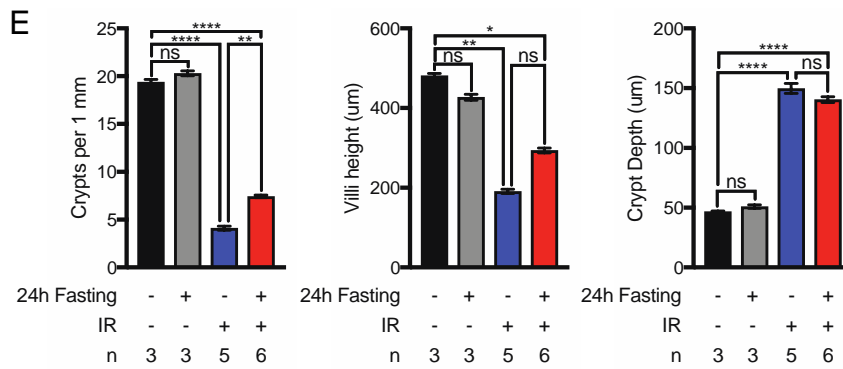
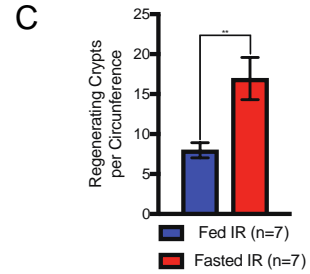
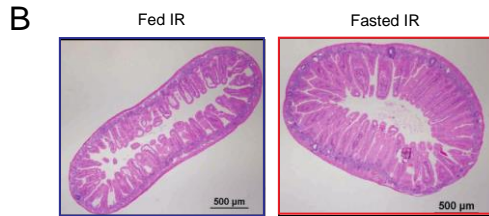
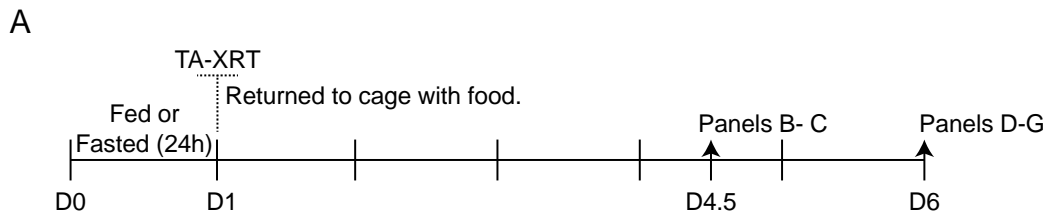
All fed mice died between days 6 and 7. In contrast, all of the animals that were fasted prior to radiation exposure survived for 30 days, the study endpoint (Fig. 3B). Fed animals decreased their food intake until time of death which occurred at day 6-7 and was due to radiation-induced toxicity. Food intake began to increase by day 7 in fasted mice, peaking at day 11 and eventually stabilizing at 4 g/day up to day 30 (Fig. 3C). Body weight decreased steadily in fed mice from original body weight until death at day 6-7. In contrast, fasted animals lost approximately 20% of their body weight during the 24 h fast period, but refeeding resulted in a 10% regain of original body weight by day 3 followed by a steady decline until day 7. By day 14, these mice had regained most of their original weight and maintained or increased it until study endpoint (Fig. 3D). Both groups showed general signs of radiation toxicity, including decreased activity, ruffled fur, and hunched back posture but at day 8, the fasted group started to revert to healthy activity levels.

Fasting protects SI stem cells, enabling recovery of SI epithelium after radiation

To examine the effects of pre-radiation fasting on intestinal stem cell regeneration after radiation we performed traditional microcolony assays (Fig. 4A and B), which demonstrated a significantly greater number of regenerating crypts per circumference in the fasted group relative to the fed group (Fig. 4C).

Figure 4 Fasting protects SI stem cells from high dose radiation.

(A) C57Bl/6J mice were treated as shown. (B) Representative images of hematoxylin and eosin (H & E)-stained SI (day 4.5). Scale bars, 500 μm . Magnification, 4x. (C) Regenerating crypts per circumference were quantified in 4 separate sections of intestine and the average per mouse was plotted. The Student *t*-test was performed for comparison of groups ($n = 7$ per group, $p=0.0077$). Error bars are \pm SEM. (D) Representative images of H & E-stained SI (day 6). Scale bars, 100 μm . Magnification, 10x. (E) Quantification of H & E data. Crypt depth and villi height ($n=50$ per mouse) were measured and plotted. Number of crypts per length ($n=30$ fields per mouse) of SI was quantified for each sample and number of crypts per millimeter of SI length plotted. * $P<0.05$; ** $P<0.005$, **** $P<0.0001$ by Tukey post-test of a one-way ANOVA. Error bars are \pm SEM. (F) Reporter mice were administered two doses of tamoxifen (t) 1 and 3 h after radiation. Mice were euthanized on D6, SI were harvested and whole-mount tissue stained for LacZ expression. Villi were removed from a 3-cm section of LacZ-stained whole-mount tissue for counting traced crypts. Representative images are shown. (Scale bars, 500 μm) (G) The number of fully traced crypts per field of view in whole-mount images was quantified, individual mice plotted. ** $P<0.005$ by Holm-Sidak's multiple comparison of a one-way ANOVA. Error bars are \pm SEM.



To further evaluate the effects of the TA-XRT field on the mice, abdominal organs were harvested from fed and fasted mice at day 6 post-radiation. SI tissues from irradiated mice showed significant damage compared to those of unirradiated mice (Fig. 4D). Specifically, SI from irradiated mice showed hypertrophic crypts and shortened villi compared to unirradiated controls. Moreover, the number of crypts per mm of intestine was significantly greater in the SI of the fasted-irradiated group than in those of the fed-irradiated group (Fig. 4E). The greater number of crypts per mm of intestine suggested that fasting protected SI stem cells.

Results from microcolony assays as well as the presence of hypertrophic crypts, suggested that fasting protected SI stem cells from high-dose radiation. Stem cell reporter mice were used to test which stem cell populations were responsible for epithelial repopulation following radiation damage. Knock-in mice carrying tamoxifen-inducible Cre under the transcriptional control of the mouse *Lgr5* promoter to mark crypt base columnar (CBC) stem cells(57) or the *Bmi1* promoter to mark the supra-Paneth (+4) stem cell pool(70) were bred to mice carrying the floxed-stop *Rosa26-LacZ* reporter (R26R) to induce permanent LacZ expression, mark *Lgr5*⁺ or *Bmi1*⁺ cells, and enable lineage tracing. Fed and fasted mice were treated with TA-XRT followed by tamoxifen at 1 and 3 h post-radiation. SI tissues were isolated on day 6, stained for LacZ expression (Fig. 4F), and traced crypts per area were quantified (Fig. 4G). Although traced crypts were observed in both *Lgr5* and *Bmi1* reporter mice, fasting only significantly increased those in *Lgr5* reporter mice.

Because mice in both fed and fasted groups exhibited radiation-induced toxicity at day 6 (Fig. 3), we evaluated intestinal tissues at different time points within the observed 30-day survival timeline to evaluate whether intestinal epithelium recovery correlated with mouse health. Intestinal tissues were harvested from both fed- and fasted-irradiated mice at day 4 as well as at days 10 and 30 from fasted-irradiated groups (Fig. 5).

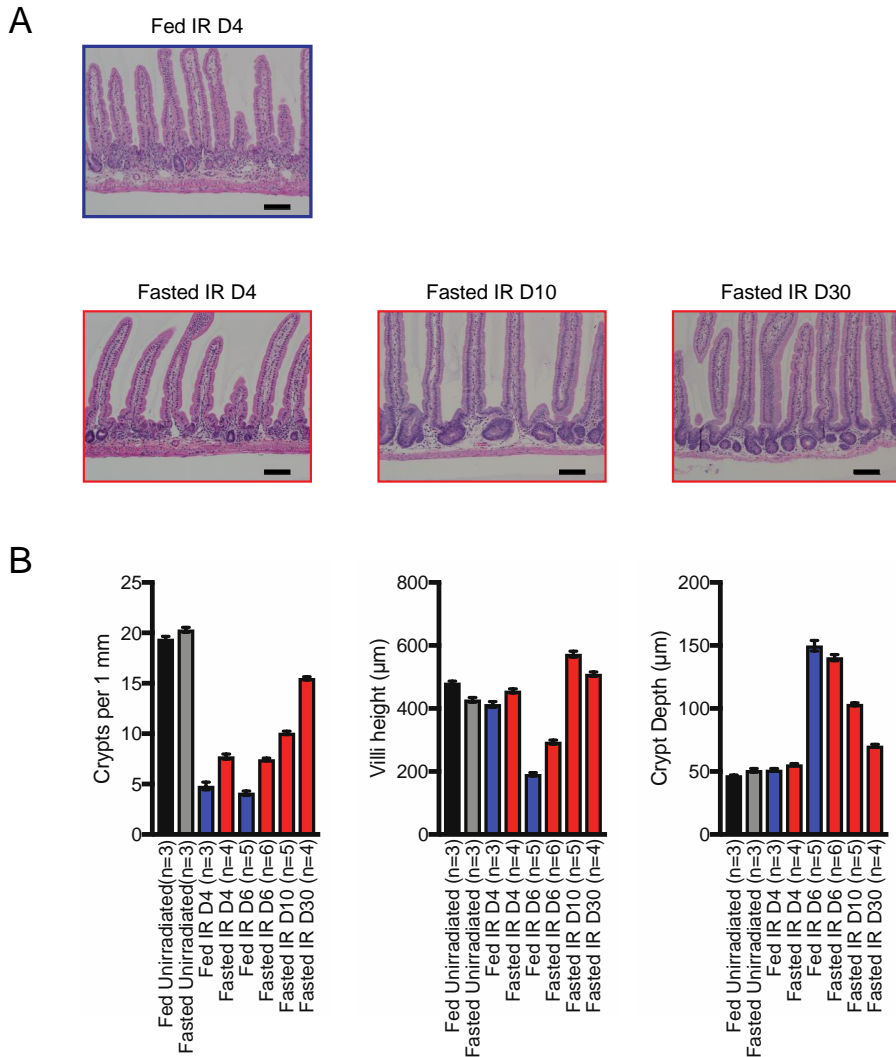


Figure 5 Fasting induced-protection of small intestinal stem cells allows for intestinal epithelium recovery after radiation.

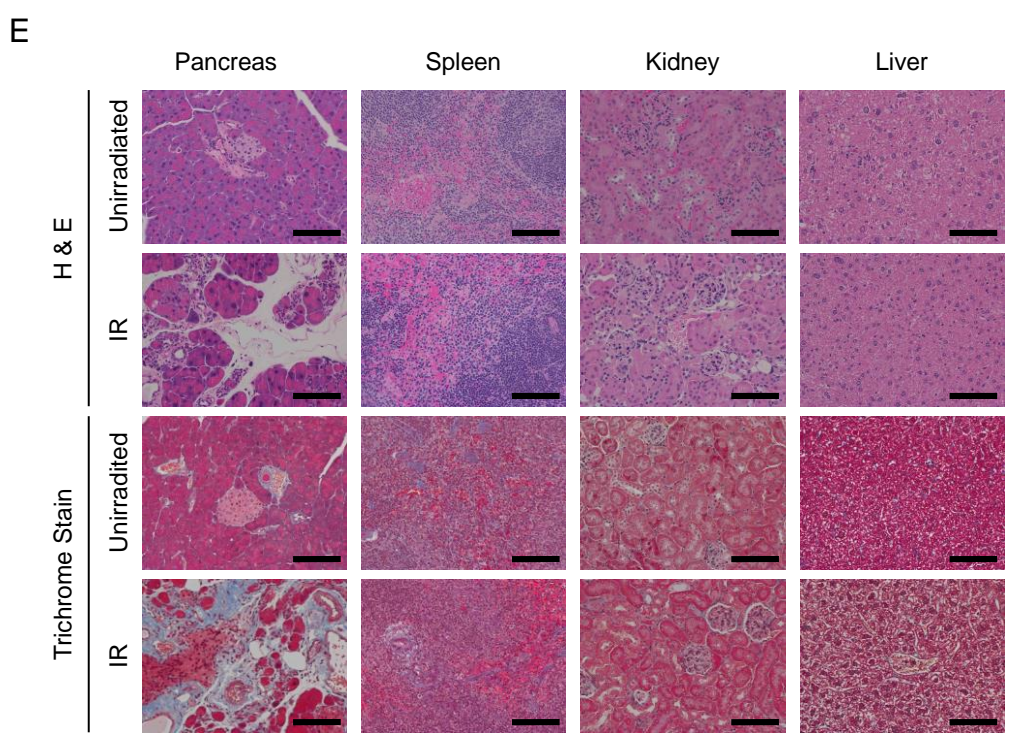
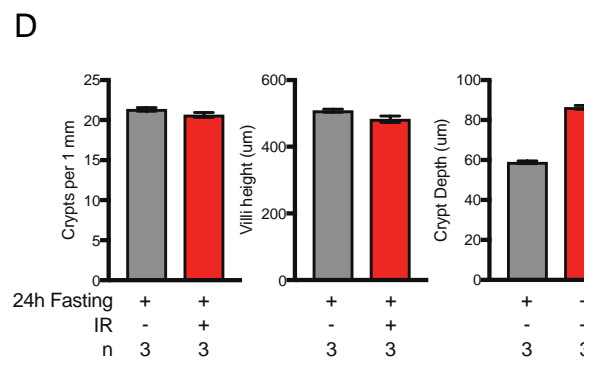
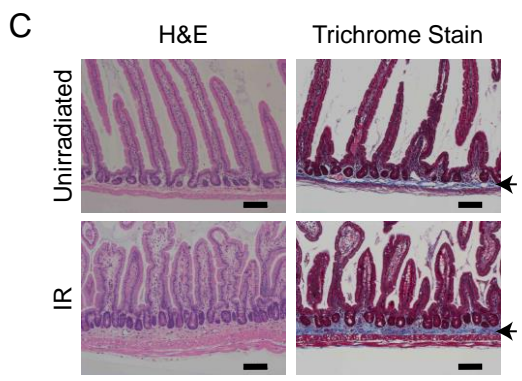
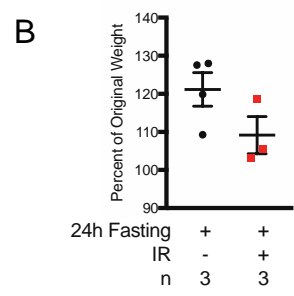
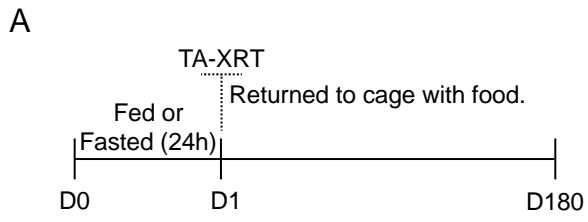
Mice were treated as described in Fig. 2 and their SI were harvested at various time points following radiation (D4, D10, D30). (A) Representative images of H & E-stained jejunum. Scale bars, 100 μm. Magnification, 10x. (B) Quantification of H & E data. Crypt depth and villi height (n = 50 per mouse) were measured and average value per treatment group plotted. Number of crypts per length of SI (n = 30 fields per mouse) was quantified for each sample and average number of crypts per millimeter of SI length plotted.

At day 4, an appreciable decrease in the number of crypts per mm was noted in the fed-irradiated group as compared to the fasted-irradiated group (Fig. 5). This decrease was maintained through day 6. Additionally, villi blunting occurred between days 4 and 6. Both these measures correlated with declining animal health in fed and fasted cohorts for up to 7 days in the fasted-irradiated group and until death in the fed-irradiated group (Fig. 3). In fasted mice, intestinal epithelium regeneration was observed by day 10, as evidenced by increased crypts per mm of intestine, increased villi length, and decrease crypt hypertrophy. Intestinal recovery at day 10 correlated with improved health in fasted-irradiated mice and their subsequent survival.

Fasted-irradiated and fasted-control mice were followed for 180 days to determine if short-term fasting protected mice from the long-term side-effects associated with high-dose radiation (Fig. 6).

Figure 6 Long term effects of high dose radiation.

A) C57Bl/6J mice were treated as shown. (B) Body weight was recorded at time of euthanasia. (C) Representative images of H & E and Trichrome-stained SI. Arrows denote intestinal submucosa. Scale bars, 100 μ m. Magnification, 10x. (D) Crypt depth and villi height (n = 50 per mouse) were measured and average value per treatment group plotted. Number of crypts per length of SI as quantified (n = 30 fields per mouse) and average number of crypts per millimeter of SI length plotted. (E) Representative images of H & E stained and Trichrome stained abdominal organs within the radiation field. Scale bars, 100 μ m. Magnification, 20x.



At D180 one mouse in the fasted-irradiated group was found deceased. The remaining mice were euthanized and their kidneys, livers, spleens, pancreata and SI were isolated. Although most fasted-irradiated mice weighed less than fasted-unirradiated mice at the time of euthanasia, the difference was not significant (Fig. 6B). Pancreatic tissue was found in only one of the three remaining fasted-irradiated mice and their SI were thicker and more rigid than those isolated from fasted non-irradiated mice. By gross examination, livers, kidneys and spleens were indistinguishable between irradiated and non-irradiated cohorts.

Next, tissue sections were stained with hematoxylin and eosin (H & E) and trichrome for microscopic evaluation. There were no significant differences in crypt depth, villi height or number of crypts per mm of SI between the fasted-irradiated and fasted-unirradiated groups indicating a recovery of the SI epithelial compartment following the original radiation insult (Fig. 6C-D). However, submucosal fibrosis was observed in the SI of fasted-irradiated mice. Microscopic evaluation of remaining pancreatic tissue from the one irradiated mouse where pancreatic tissue could be found, revealed fibrosis and loss of exocrine pancreas. By contrast, fibrosis was not detected in the spleens, kidneys or livers of fasted-irradiated mice (Fig. 6E).

Separate cohorts of fed or fasted mice that had been radiated or not were euthanized and their SI harvested at different timepoints and stained with antibodies specific for γ H2AX and CC3 to evaluate DNA damage and cell death (Fig. 7).

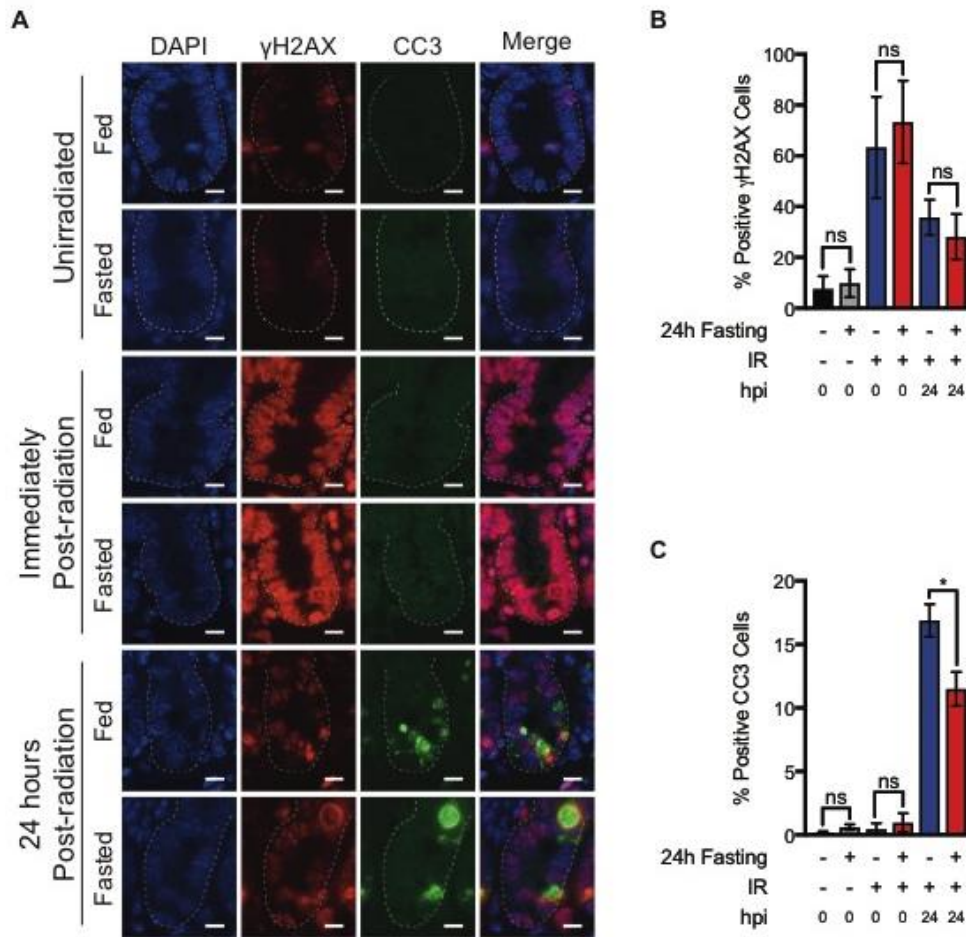


Figure 7 Effects of pre-radiation fasting on IR-induced DNA damage and apoptosis.

(A) C57Bl/6J mice were allowed to feed *ad libitum* or were fasted for 24 h. Unirradiated SI tissues were harvested at this time. Other cohorts were radiated with TA-XRT (11.5Gy) and SI tissues harvested either immediately or 24 h after radiation (hpi= hours post irradiation). SI tissues (jejunum) were analyzed for γ H2AX and cleaved caspase-3 (CC3) by immunofluorescence staining. Representative images are shown. Scale bars, 10 μ m. Magnification, 20x. (B) Positive γ H2AX cells per crypt were quantified (30 crypts per mouse, n=4 mice per treatment group and mean per treatment plotted. ns= not significant by student's t-test. Error bars are \pm SEM. (C) Positive cleaved caspase-3 cells per crypt were quantified (30 crypts per mouse, n=4 mice per treatment group and mean per treatment plotted. ns= not significant; *P<0.05 by student's t-test. Error bars are \pm SEM.

There were no significant differences in the number of crypt epithelial cells staining positive for γ H2AX between fed and fasted cohorts at any of the evaluated timepoints (Fig. 7B). These results indicate that in SI crypts, fasting on its own did not induce DNA damage, nor did it significantly impact the generation or resolution of DNA damage following radiation. Although there were no differences in the number of crypt epithelial cells staining positive for γ H2AX in fed and fasted mice 24h post-radiation (Fig. 6B), there were reduced levels of CC3 staining in the crypts of fasted mice (11.492% positive crypt cells) when compared to fed mice (16.891% positive crypt cells) (Fig. 7C). These results indicate that fasting may protect SI crypt cells from IR-induced apoptosis or that apoptotic cells were cleared more readily in fasted animals. There were no significant differences in Ki67 staining between fed or fasted cohorts at any of the evaluated timepoints (Fig. 8).

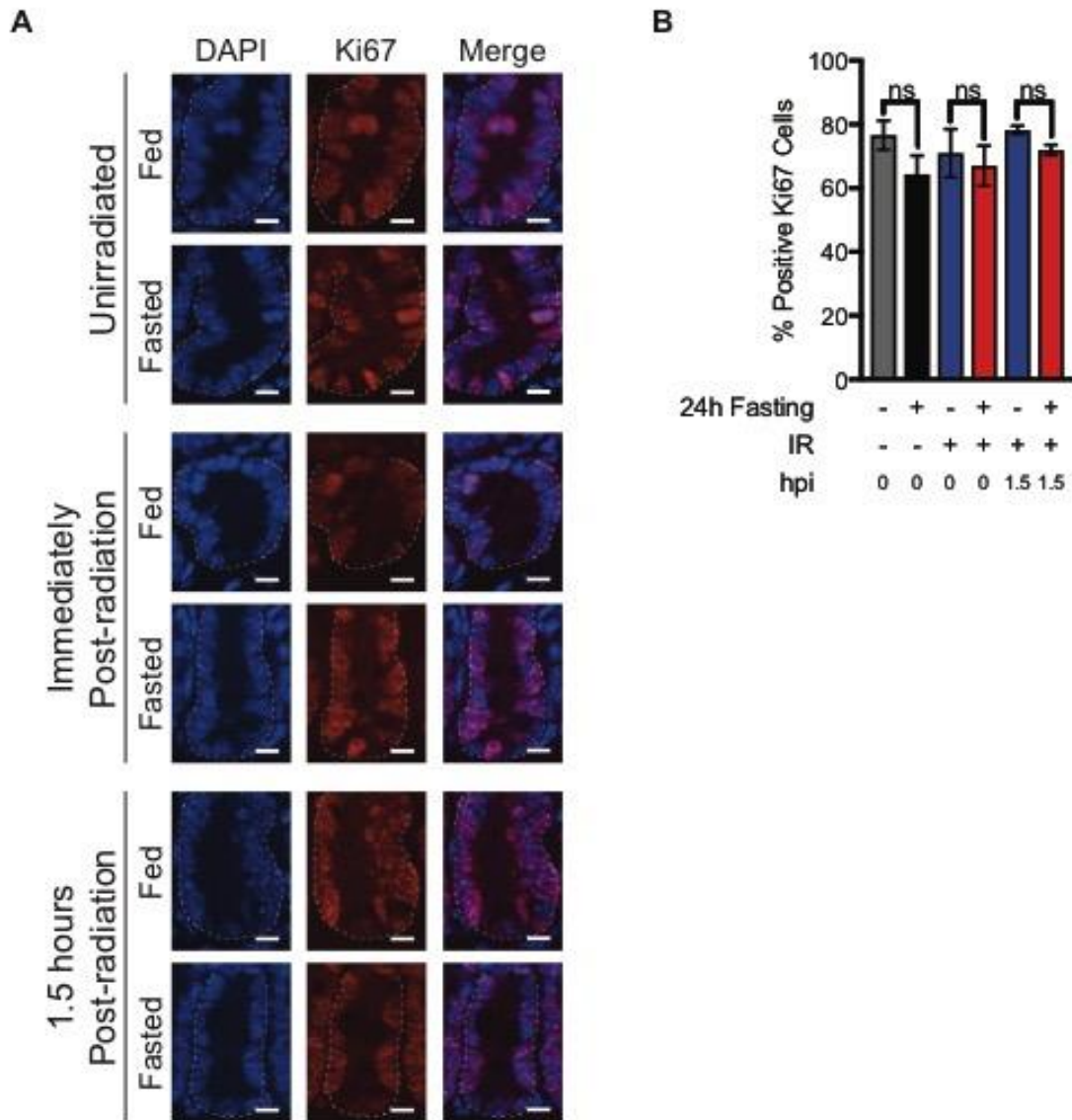


Figure 8 Twenty-four hour fasting did not reduce the number of crypt epithelial cells staining positive for Ki67 relative to fed controls.

(A) C57Bl/6J mice were allowed to feed *ad libitum* or were fasted for 24h. Unirradiated SI tissues were harvested at this time. Other cohorts were radiated with TA-XRT (11.5 Gy) and SI tissues harvested either immediately or 1.5 h after radiation (hpi= hours post irradiation). Tissues were analyzed for Ki67 by immunofluorescence staining. Representative crypt images shown. Scale bars, 10 μ m. Magnification, 20x. (B) Ki67 positive cells per crypt were quantified (30 per mouse, n=3-4 mice per treatment group) and average per treatment plotted. ns= not significant by student's t-test. Error bars are \pm SEM.

Pre-radiation fasting does not reduce tumor response to radiation

The response of malignant and normal cells to genotoxic stress is differentially affected by fasting(26, 35, 38). Fasting chemosensitizes tumors(26, 35, 38) while protecting normal tissues against toxicity. To determine the effects of fasting on the radiation responses of pancreatic cancer, we employed a syngeneic orthotopic KPC model of pancreatic cancer, using cells with a heterozygous *Trp53* loss-of-function mutation and an activated *Kras* allele(87). KPC cells were implanted into the pancreata of C57BL/6J mice, and tumors became established over 2 weeks as detected by ultrasound imaging (Fig. 9 and Fig. 10A).

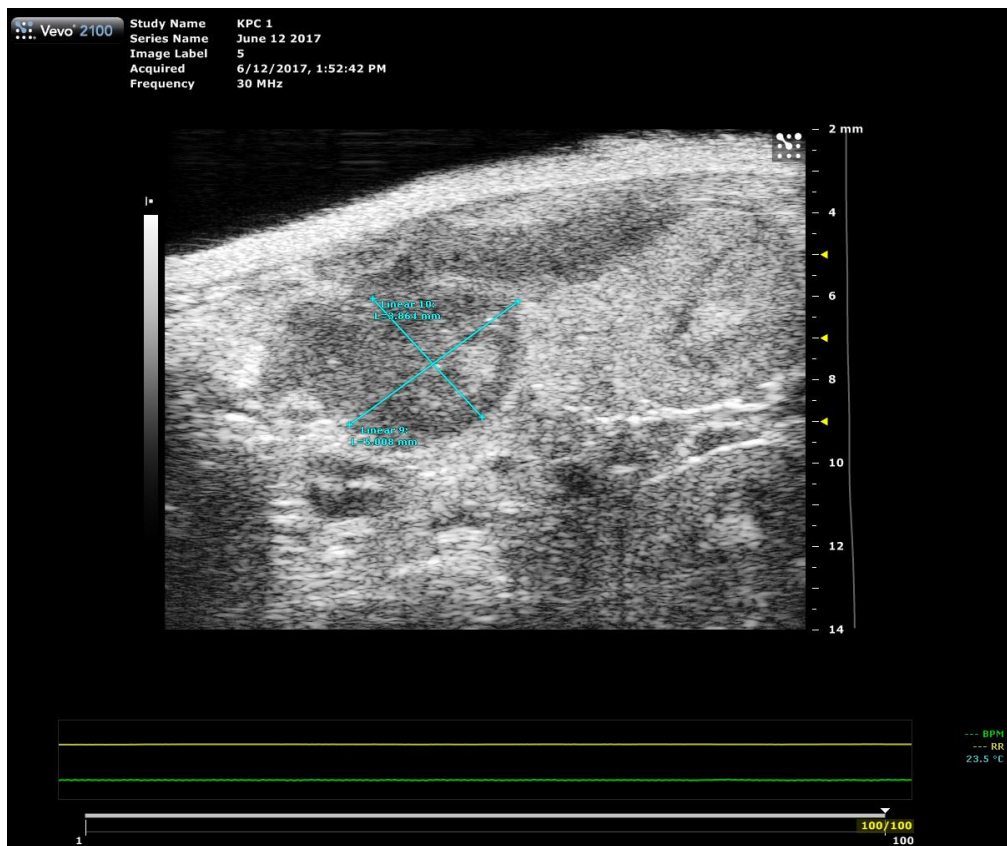


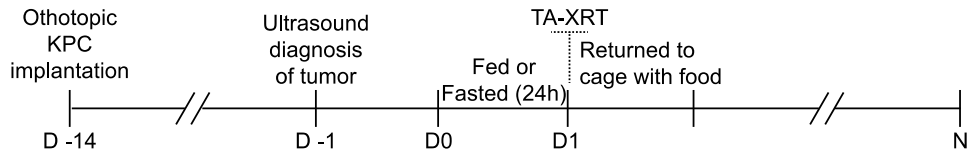
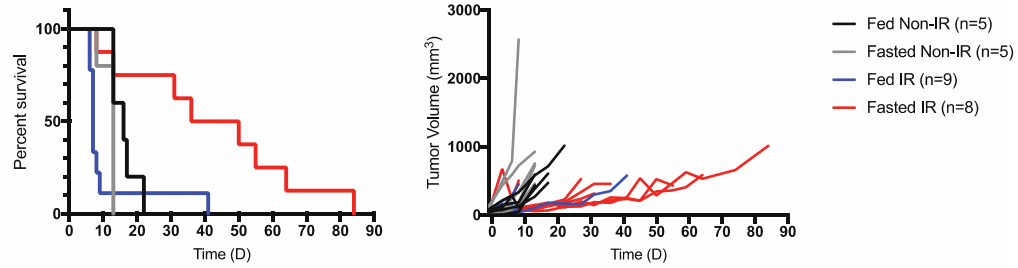
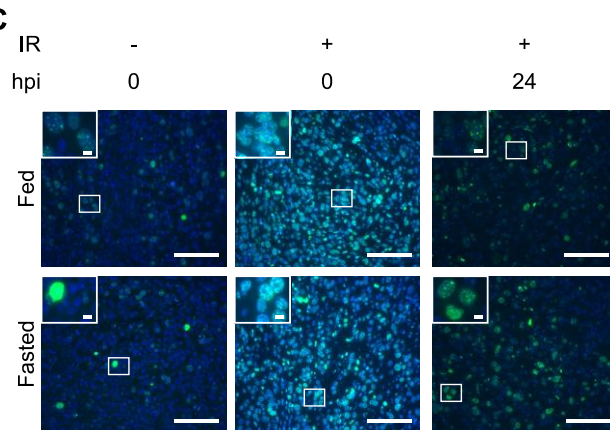
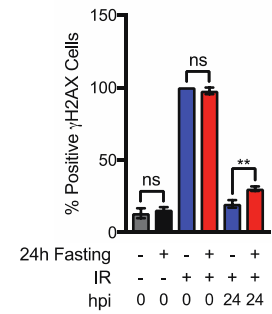
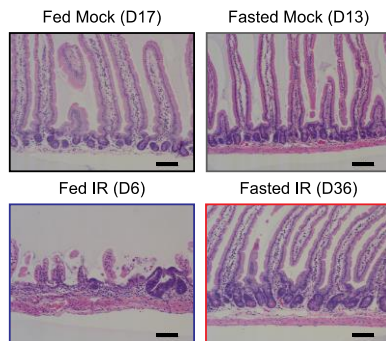
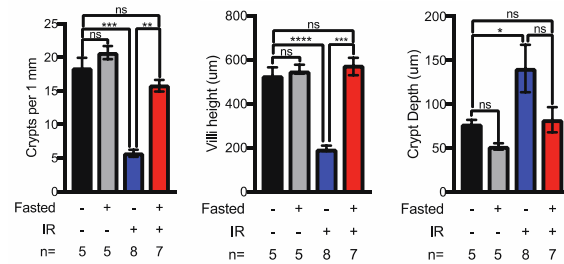
Figure 9 Diagnostic ultrasounds of pancreatic tumor.

Representative ultrasound image of orthotopically-implanted pancreatic tumor. Blue lines denote tumor diameter measurements.

After tumors were confirmed, animals were randomized to four treatment groups: fed-unirradiated, fasted-unirradiated, fed-irradiated, and fasted-irradiated. Mice were either fed or fasted for 24 h, then irradiated with a single dose of TA-XRT (12 Gy) or not, and returned to their cages with food. Ultrasound imaging was performed every 4-5 days to monitor tumor growth and animals were euthanized due to excessive tumor burden or an observed general health decline, as per IACUC guidelines (Fig. 10A).

Figure 10 Pre-radiation fasting does not confer protection to orthotopic KPC pancreatic tumors.

(A) KPC cells (2×10^5) were orthotopically injected into 12-week-old C57Bl/6J mice. Two weeks later, tumors were measured using ultrasound and mice were randomized into four treatment groups. Mice were allowed to feed or were fasted for 24 h. Total abdominal radiation (TA-XRT; 12 Gy) was administered (day 1). Access to food was restored immediately after treatment. Ultrasound tumor measurements were taken every 4-5 days until death. (B) Survival was monitored daily. Tumor growth curves for individual mice are shown. Bonferroni corrected Log-rank test. (C) Pancreatic tumor-bearing mice were treated as indicated (hpi = hours post irradiation) and tumors were analyzed for γ H2AX by immunofluorescence staining. Representative images are shown. (D) Positive cells per field were quantified (5 fields per mouse, n=3 mice per treatment) and average per treatment was plotted. Scale bars, 100 μ m. Magnification, 40x. Inset scale bars, 20 μ m. **P<0.005 by Tukey post-test of a two-way ANOVA. Error bars are \pm SEM. (E-F) Representative images of H & E-stained jejunum from tumor-bearing mice harvested at the time of euthanasia (as indicated). Scale bars, 100 μ m. Magnification, 10x. Crypt depth and villi heights (n = 50 per mouse) were measured and average value per treatment group plotted. Number of crypts per length of SI as quantified for each sample (n=30 fields per mouse) and average number of crypts per millimeter of SI length plotted. *P<0.05; **P<0.005, ***P<0.0005, ****P<0.0001 by Tukey post-test of a one-way ANOVA. Error bars are \pm SEM.

A**B****C****D****E****F**

Fasting alone did not significantly affect the median survival of unirradiated tumor-bearing mice (Fig. 10B). When combined with TA-XRT, fasting significantly increased median survival (to 43 days) when compared to fed-irradiated tumor-bearing mice (7 days, Log rank $P=0.0021$) and modestly increased median survival when compared to fasted-unirradiated tumor-bearing mice (13 days, Log rank $P=0.0231$, Fig. 9B). Tumors in the fasted-irradiated group consistently showed a lag in growth following radiation, thereby prolonging survival in this group (Fig. 10B and 11).

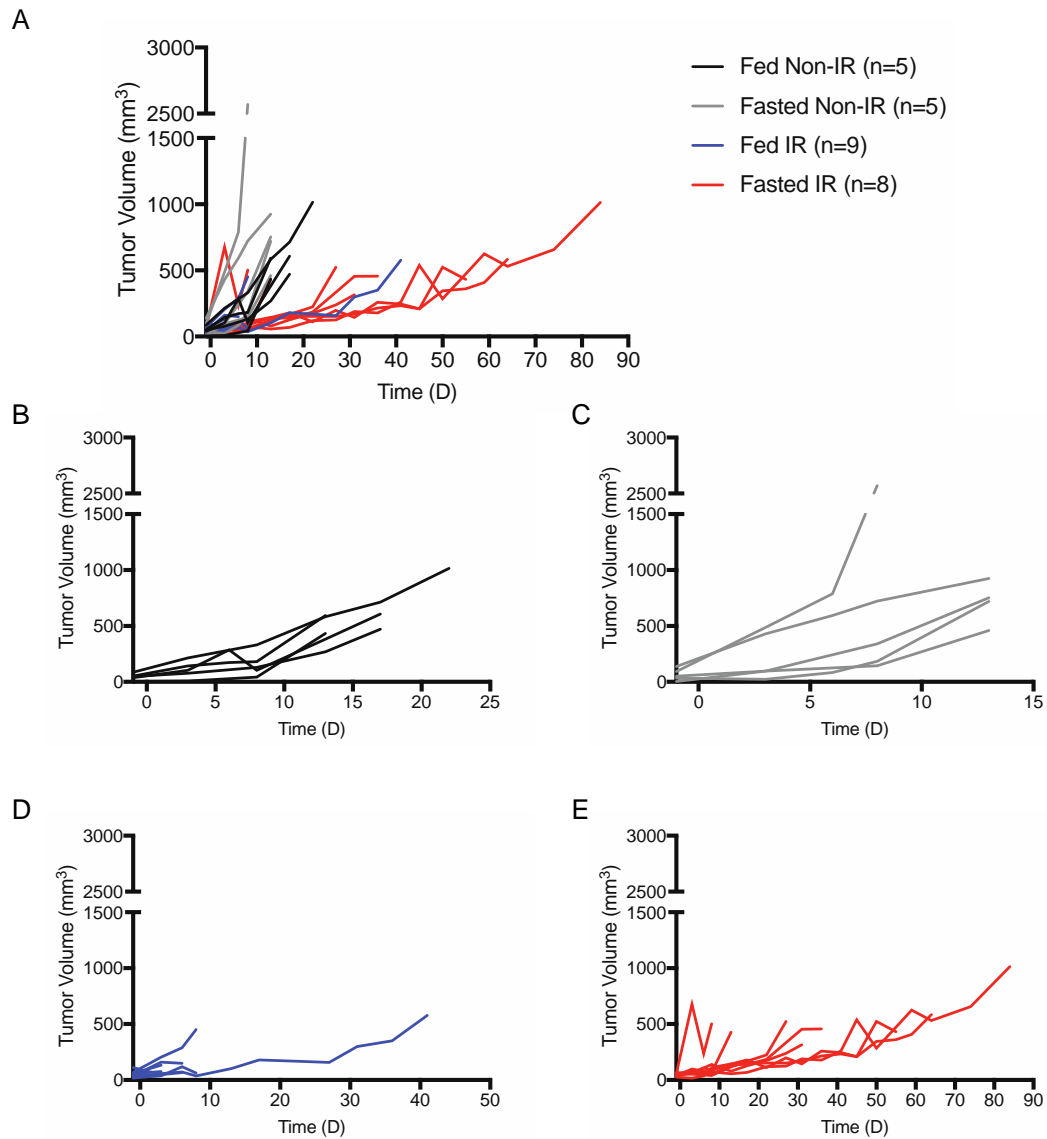


Figure 11 Individual tumor growth curves.

KPC cells (2×10^5) were orthotopically injected into 12-week-old C57Bl/6J mice. Two weeks later, tumors were measured using ultrasound and mice were randomized into four treatment groups. Mice were allowed to feed or were fasted for 24 h. Total abdominal radiation (TA-XRT; 12 Gy) was administered (day 1). Access to food was restored immediately after treatment. Ultrasound tumor measurements were taken every 4-5 days until death. Tumor growth curves for individual mice are shown.

To further evaluate the effects of fasting on tumor cells treated with radiation, we grew orthotopic KPC tumors and subjected the mice to fed or fasted conditions after tumors had grown to an efficient size for measurements. Mice were then irradiated or not and tumors were harvested either immediately or 24 h post-radiation. Tumor tissues were stained with antibodies specific for either γ H2AX (Fig. 10C) or CC3 (Fig.12).

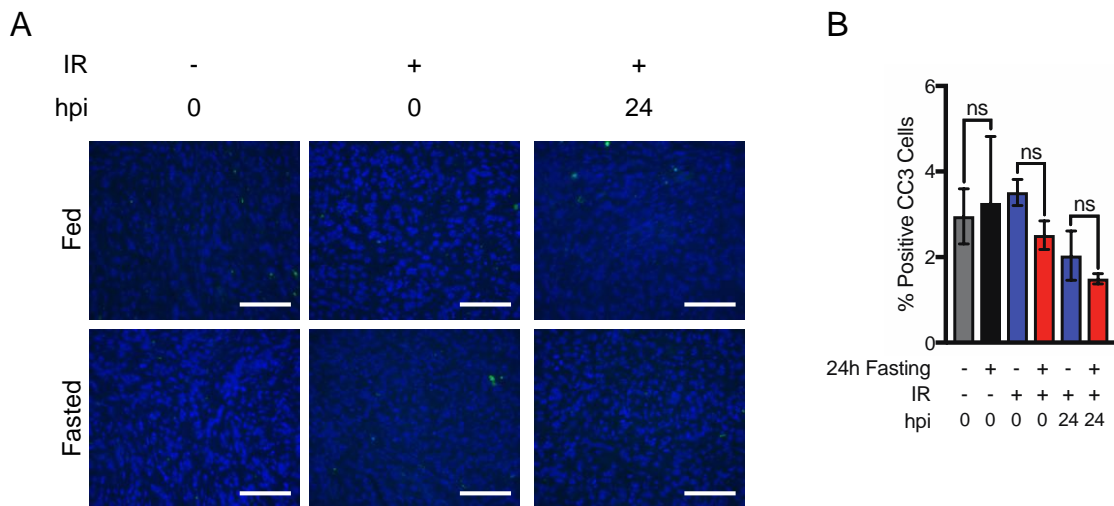


Figure 12 Pancreatic tumor viability in fed or fasted states following IR

(A) Pancreatic tumor-bearing mice were treated as indicated (hpi = hours post irradiation) and tumors were analyzed for cleaved caspase-3 (CC3) by immunofluorescence staining. Representative images shown. (B) Positive cells per field were quantified (5 fields per mouse, n = 3 mice per treatment) and average per treatment plotted. Scale bars, 100 μ m. Magnification, 40x. ns= not significant by Tukey post-test of a two-way ANOVA. Error bars are \pm SEM.

Baseline levels of γ H2AX were similar in fed and fasted-unirradiated tumors. Tumors harvested from fed and fasted mice immediately after radiation had similarly high levels of γ H2AX. Together these results suggested that fasting alone did not induce DNA damage nor reduce the capacity of radiation to induce DNA damage in tumors. Moreover, levels of γ H2AX were significantly higher in the 24 h post radiation

tumors of fasted mice relative to their fed cohorts (Fig. 10D) indicating that fasting prior to radiation reduced the capacity of pancreatic tumors to repair the DNA double strand breaks induced by IR. There were no significant differences in CC3 levels between fed and fasted tumors at any time point (Fig. 12).

SI were isolated from tumor bearing mice at the time of euthanasia to examine tissue integrity (Fig. 10E). Fed-irradiated mice that died within 10 days of irradiation (8/9 mice, 88.9%) showed severely atrophic SI epithelia (Fig, 10E). There were fewer crypts per mm of jejunum, blunted villi, and more hypertrophic crypts compared to unirradiated controls and fasted-irradiated mice (Fig 10F). In contrast, fasted-irradiated mice that survived initial radiation-induced toxicity (7/8, 87.5%), displayed abundant crypts per mm and healthy-looking villi. In comparison, SI from unirradiated controls were normal (Fig. 10E and F).

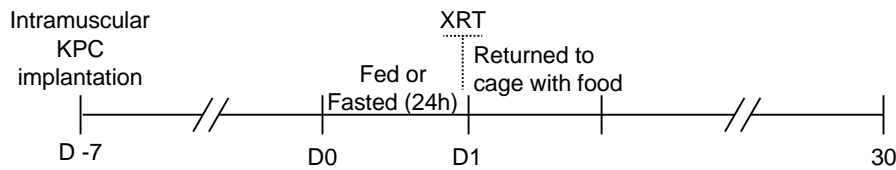
Because most of the animals in the fed-irradiated group were euthanized due to radiation-induced GI toxicity (Table 1), the effect of fasting on tumor response to radiation could not be fully examined.

Table 1 Recorded cause of death in tumor-bearing mice

Fed/ Fasted	IR/ Unirradiated	Day of Death	Recorded cause of death
Fed	Unirradiated	16	Euthanized due to excessive tumor burden
Fed	Unirradiated	13	Euthanized due to excessive tumor burden
Fed	Unirradiated	13	Euthanized due to excessive tumor burden
Fed	Unirradiated	22	Euthanized due to excessive tumor burden
Fed	Unirradiated	17	Unknown
Fasted	Unirradiated	8	Euthanized due to excessive tumor burden
Fasted	Unirradiated	13	Euthanized due to excessive tumor burden
Fasted	Unirradiated	13	Euthanized due to excessive tumor burden
Fasted	Unirradiated	13	Euthanized due to excessive tumor burden
Fasted	Unirradiated	13	Euthanized due to excessive tumor burden
Fed	IR	7	Euthanized due to radiation toxicity
Fed	IR	8	Euthanized due to radiation toxicity
Fed	IR	7	Euthanized due to radiation toxicity
Fed	IR	9	Euthanized due to radiation toxicity
Fed	IR	41	Euthanized due to excessive tumor burden
Fed	IR	7	Euthanized due to radiation toxicity
Fed	IR	7	Euthanized due to radiation toxicity
Fed	IR	6	Euthanized due to radiation toxicity
Fed	IR	6	Euthanized due to radiation toxicity
Fasted	IR	64	Euthanized due to general decline of health
Fasted	IR	84	Euthanized due to general decline of health
Fasted	IR	36	Euthanized due to excessive tumor burden
Fasted	IR	55	Unknown
Fasted	IR	8	Euthanized due to radiation toxicity
Fasted	IR	31	Euthanized due to excessive tumor burden
Fasted	IR	13	Euthanized due to excessive tumor burden
Fasted	IR	50	Euthanized due to general decline of health

Therefore, we utilized an intramuscular tumor model in which KPC tumor cells were injected in the hind leg of mice (Fig. 13).

A



B

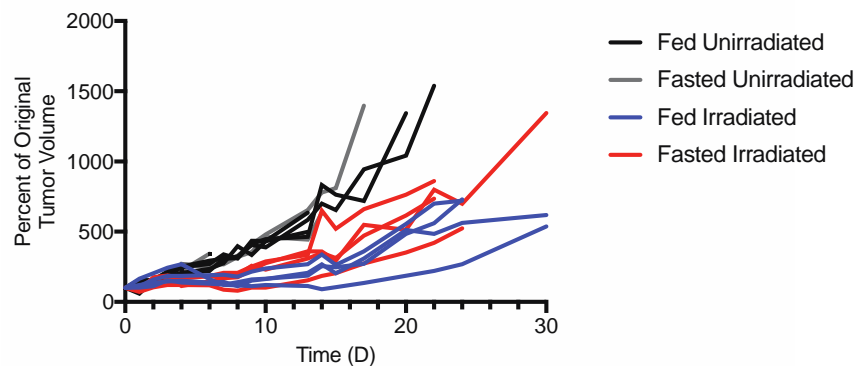


Figure 13 Pre-radiation fasting does not confer protection to KPC tumors.

(A) Overall schema and timeline. To test the effect of fasting on tumor response to radiation, KPC pancreatic cancer–derived (K8484) cells syngeneic with C57Bl/6J (1×10^6) were injected into the hind leg of 8-week-old C57Bl/6J mice. Mice were randomized to one of four treatment groups as indicated and treatment began 6 days after implantation. Mice were either fed or fasted for 24 h (day 0) and then not irradiated or subjected to irradiation of the hind leg with a single dose of 16 Gy radiation (day 1). Animals were returned to single-housed cages with food. (B) Tumors were measured with calipers daily for the first 2 weeks and every other day thereafter. Mice were euthanized when tumors reached 15 mm in any dimension. Individual tumor growth curves were plotted.

By radiating only the hind limb, we eliminated competing death from GI toxicity. Although radiation caused a minor lag in tumor growth when compared to unirradiated controls, there were no significant differences in tumor growth between the fed and fasted groups (Fig. 13).

Discussion

In this study, we describe how a 24 h fast promoted intestinal stem cell regeneration and organismal survival after a lethal dose of abdominal radiation. This protection appears to be limited to normal tissues, as pancreatic tumors were not radioprotected and may have even demonstrated a mild, but selective increase in radiation damage, as measured by γ -H2AX foci. The mechanism of this effect may be from reduced early apoptosis in normal tissues, but not tumors.

We developed a novel TA-XRT model using a 25 mm circular collimator that targeted intestinal tissue while sparing most of the bone marrow in the thorax and pelvis. This enabled us to impart GI toxicity without invoking competing hematopoietic toxicity. We note that very little toxicity was observed in mice that survived otherwise lethal radiation, with limited intestinal and pancreatic fibrosis. We also used this large field to treat pancreatic tumors, which led to improved outcomes only when coupled with a short term fast for radioprotection. Thus, despite these excellent outcomes, we note that these experiments only demonstrate proof of principle for fasting-mediated radioprotection to enable ablative RT. Future clinical studies should use smaller fields such as those used in stereotactic body radiotherapy (SBRT), which would further reduce both acute and chronic radiation-induced sequelae.

Two distinct stem cell populations have been thoroughly described in the SI. Lgr5+ stem cells reportedly replenish the SI epithelium during homeostatic turnover of villi cells(57) while Bmi1+ stem cells are more quiescent under normal physiological conditions(70). After radiation, Bmi1+ stem cells proliferate and have the capacity to produce Lgr5+ stem cells and repopulate the SI epithelium(70). It has also been

shown that although Lgr5⁺ stem cells are radiosensitive, complete depletion prior to radiation impairs intestinal epithelial recovery. This suggests that Lgr5⁺ stem cells are also required for crypt epithelial cell regeneration post damage(88). In the context of fasting-mediated SI radioprotection, we provided evidence that both Lgr5⁺ and Bmi1⁺ intestinal stem cells contributed to regeneration of the SI following high dose radiation.

Additional studies have also shown that other intestinal cell types including Dll1⁺ secretory progenitors(89), label retaining cells(90), Alpi expressing enterocyte precursors(91), Krt19⁺ progenitor cells(92), enteroendocrine(93), and Paneth cells(94, 95) are capable of de-differentiating when the stem cell compartment is compromised. Furthermore, a recent study employing single cell RNA sequencing identified a novel multipotent SI stem cell, deemed revival stem cells, marked by high clusterin expression that undergoes transient expansion following irradiation. These revival stem cells were shown to reconstitute the Lgr5 compartment following ablation with diphtheria toxin and to facilitate intestinal regeneration after experimentally-induced colitis(96). Future studies should interrogate the contribution made by each these cell populations to crypt epithelial cell recovery following ionizing radiation under fed and fasted conditions. Furthermore, experiments should investigate the generalizability of our SI observations to other stem cell niches like skin and bone marrow.

Several clinical trials have monitored the effects of fasting on the response of cancer patients to therapy. One study randomized women with stage II/III breast cancer into a short-term fast 24 h before and after the start of their chemotherapy regimen or a control arm of regular nutrition. In this study, short term fasting was well tolerated and reduced chemotherapy-induced hematological toxicities(97). Another

study evaluated different fasting periods, from 24-72 h, prior to platinum-based chemotherapy. Decreased DNA damage was observed in the leukocytes of patients who fasted over 48 h. This study also showed that fasting up to 72 h was feasible and induced minor side-effects including fatigue, headache, and dizziness(98).

It has been approximated that a 24 h fast in mice correlates to a one week water-only diet in humans(86). Many patients who receive SBRT already fast for extended periods of time to reduce filling of the stomach and duodenum(99). However, we do not envision that fasting beyond 24 hours would be advisable in pancreatic cancer patients, many of whom are already underweight and/or cachectic. Identifying the molecular mechanisms underlying the potent and selective radioprotection afforded by fasting could lead to the identification of a drug mimetic that could be employed instead of having to persistently reduce dietary intake in this already frail patient population.

Fasting-induced downregulation of IGF-1 has been proposed as one mechanism to explain how fasting provides chemoprotection to normal but not tumor tissue(26). IGF-1 deficient mice survive longer than wild-type when exposed to lethal doses of a variety of chemotherapies including cyclophosphamide, 5-fluorouracil and doxorubicin(26). Contrary to these observations, reduction in the circulating levels of IGF-1 was shown to sensitize, rather than protect, non-tumor bearing mice to etoposide treatment(26). Fasting-mediated protection from lethal doses of etoposide is driven, in part, by increased SI stem cell survival, which correlates with their enhanced ability to repair DNA double strand breaks(71). It has also been demonstrated that caloric restriction, a prolonged reduction in caloric intake, augments

the repair of sublethal damage in normal tissues(100). Caloric restriction has been shown to upregulate proteins involved in non-homologous end joining (NHEJ) like XLF and Ku(40, 101). Additionally, the deacetylase SIRT1, which binds and deacetylates Ku70 thereby enhancing DSB repair, has been shown to have increased activity during caloric restriction. While in our data evaluating whole crypts, we did not observe significant changes in DNA damage resolution, we cannot discard the possibility that differences between fed and fasted animals would be detected if we assayed specific stem cell populations (for example Lgr5+ or Bmi1+ stem cells) since these cells compose a minority of the cells in the crypt.

Future studies should aim to identify molecular mechanisms of fasting-induced GI protection from chemotherapy and radiation therapy. A detailed understanding of the biological changes that occur in stem cells during fasting and after genotoxic stress could help identify candidate drugs to mimic fasting-induced protection.

Chapter 4: Stem cell enriched-epithelial spheroid cultures for rapidly assaying small intestinal radioprotectors and radiosensitizers *in vitro*

This chapter is based upon “de la Cruz Bonilla, M., Stemler, K. M., Taniguchi, C. M., & Piwnica-Worms, H. (2018). Stem cell enriched-epithelial spheroid cultures for rapidly assaying small intestinal radioprotectors and radiosensitizers in vitro. *Scientific Reports*, 8(1), 15410. <https://doi.org/10.1038/s41598-018-33747-7>”

Abstract

Radiation therapy is one of the main treatment options for many cancer patients. Although high doses of radiation may maximize tumor cell killing, dose escalation is limited by toxicity to neighboring normal tissues. This limitation applies particularly to the small intestine, the second most radiosensitive organ in the body. Identifying small intestinal (SI) radioprotectors could enable dose escalation in the treatment of abdominopelvic malignancies. However, the only assay currently available to identify effects of radiomodulating drugs on the regenerating capacity of SI stem cells is the Withers-Elkind microcolony assay, which requires large numbers of mice, making it a costly and low throughput method. Here, we describe a novel spheroid formation assay (SFA) that utilizes SI stem cell-enriched three-dimensional epithelial spheroid cultures to identify gastrointestinal radiomodulators *ex vivo*. The SFA is scalable for high throughput screening and can be used to identify both radioprotectors and radiosensitizers.

Introduction

Gastrointestinal (GI) toxicity often limits the amount of chemotherapy and radiation that can be given to cancer patients. This issue is highlighted with radiation therapy, which can kill solid tumors anywhere in the body but also damages adjacent normal tissue. For instance, cancers of the abdomen and pelvis, such as pancreatic and prostate adenocarcinoma, are difficult to ablate with radiation alone because these tumors require high doses of radiation for control, but are often adjacent to very radiosensitive structures of the GI tract, such as the small intestine(75). This potential for morbid toxicity, often prevents these tumors from receiving a definitive therapeutic dose. In addition, chemotherapeutic agents, such as irinotecan and anti-angiogenic biologics such as bevacizumab, also have dose limiting GI toxicities, including potentially fatal diarrhea and bowel perforation(77, 78).

Despite the fact that toxicity to the GI tract is a significant clinical problem, there are no existing approved normal tissue protectors that can prevent this toxicity. Amifostine is the only FDA approved radiation protector, but its use is limited by severe side effects such as hypotension and nausea(66). Thus, identification of novel radioprotectors could not only improve patients' quality of life by reducing the aforementioned side effects, but also increase the therapeutic window to enable dose escalation of cytotoxic therapy and more effective tumor cell killing. The classical assay to assess the cellular radiation response is the clonogenic assay, or colony formation assay, which monitors the ability of a single tissue culture cell to grow into a colony after administration of radiation or chemotherapy(67). Unfortunately, the

discovery of novel protective drugs by this assay is limited by the technical difficulties of culturing normal tissues *ex vivo*. Cell lines such as Caco-2 (colon cancer derived cells) or Hs 1.Int (non-epithelial intestinal derived cells) have been used to approximate intestinal function, but are often inadequate for estimating the ability to respond to radiation since neither of them are truly representative of normal cells(68).

The gold standard for studying the response of the intestinal tract to cytotoxic insult is the microcolony assay developed by Withers and Elkind(69), which assesses regenerating intestinal stem cells after cytotoxic therapy. This method utilizes a single lethal or sublethal administration of cytotoxic therapy (e.g. radiation) that kills existing intestinal stem cells in the crypt. Nascent stem cells that regenerate after the cytotoxic insult are identified by a histopathological technique that requires transverse sections of intestine on a single slide, which can be technically demanding(69). Even if the slides are prepared properly, the individual regenerating crypts must be counted manually by an experienced pathologist. Lastly, implicit in this assay is that each data point requires large numbers of mice, making the entire process both costly and low throughput for identifying and characterizing new modulators of intestinal damage.

The advent of intestinal stem cell enriched-spheroids grown from murine or human tissue *ex vivo* has enabled the study of normal intestinal tissue and its responses to radiation(70) or chemotherapy(71). These cultures, which are amenable to genetic modification(72), can be passaged indefinitely using growth factor-enriched media in a 3D matrix. In this study, we describe the development of a modified colony

formation assay, which we refer to as a spheroid formation assay (SFA), that establishes a small intestinal (SI) stem cell-enriched spheroid cell line directly from mice to study the effects of radiation or chemotherapy treatments *ex vivo*.

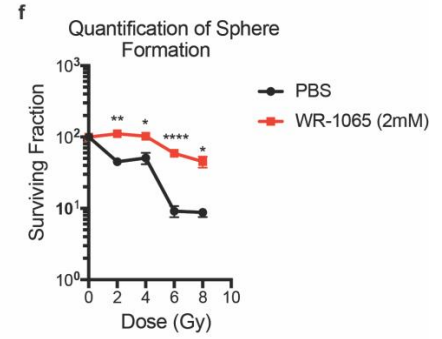
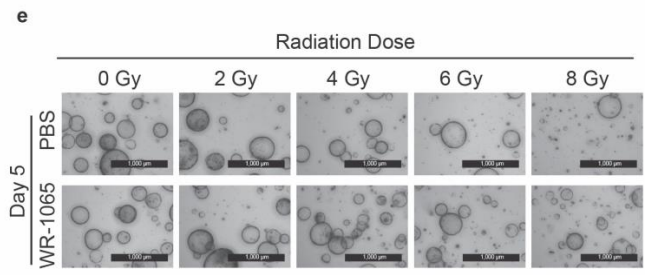
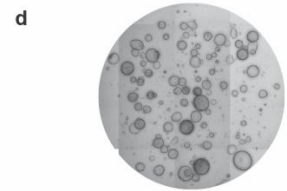
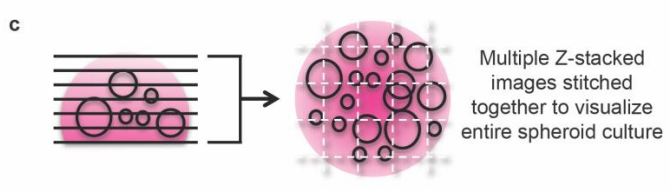
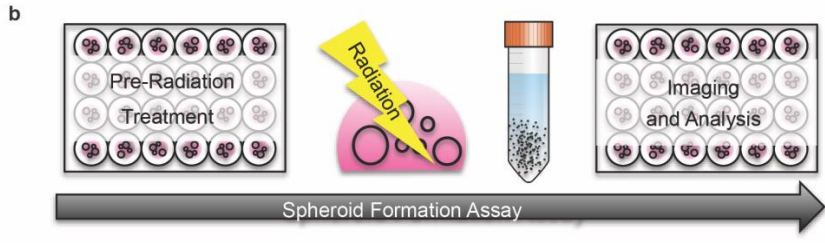
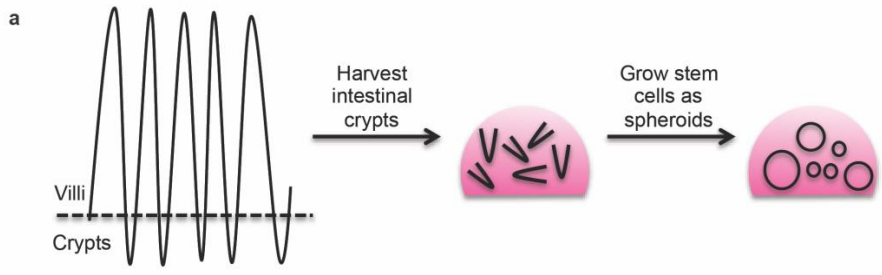
Results

Development of the Spheroid Formation Assay (SFA)

Epithelial spheroid cultures were generated from small intestinal (SI) crypts of C57BL/6J mice (Fig. 14a).

Figure 14 Spheroid formation assay to identify GI radioprotectors.

Schematic representation illustrating how stem cell-enriched epithelial spheroid cultures are established (panel a). Schematic outlining how the spheroid formation assay (SFA) is performed (see text for details, panel b). Z-stack images of treated stem cell-enriched epithelial spheroid cultures are stitched together to visualize spheroids (panel c). A representative image of the stitched z-stack is shown (panel d). Stem cell-enriched epithelial spheroid cultures treated with vehicle (PBS) or 2 mM WR-1065 for 2 h were exposed to the indicated doses of ionizing radiation. Spheroids were immediately dissociated into single cells, replated in Matrigel and imaged 5 days later (panel e) (Scale bars, 1000 μm). Spheroids larger than 150 μm in diameter were quantified and mean surviving fraction is plotted. * $P < 0.05$ by two-tailed, ** $P < 0.01$, *** $P < 0.001$, **** $P < 0.0001$ by two-tailed, Student's t test (N = 3 per group). Error bars are \pm SEM.



Protocols for isolating and culturing stem cell-enriched epithelial spheroid cultures have been described(72). Briefly, mice were euthanized according to an approved animal protocol, and their SI crypts isolated and embedded in basement membrane matrix (Matrigel). Cultures were incubated at 37°C for 2 to 4 days to allow primary spheroids to form. Primary spheroids were passaged at least 10 times at 3 day intervals which allowed for the elimination of mesenchymal cell contaminants, enrichment and expansion of non-budding stem cell enriched spheroids, and provision of enough starting material for subsequent experiments. To perform the SFA, spheroids were subjected to the desired experimental treatment, irradiated at the specified doses, isolated from the Matrigel, digested to single cell suspensions, re-plated at a pre-determined concentration, and cultured to re-establish spheroids (Fig. 14b). Cell viability was monitored as a function of time.

SFA assay for identifying radioprotectors

As a proof of concept, spheroid cultures were treated with a known radioprotector to test if the SFA would indeed reflect protection of spheroids after irradiation (i.e. increased spheroid formation after irradiation versus unprotected controls). Amifostine is a validated radioprotector and serves as a prodrug that is actively dephosphorylated to generate WR-1065, the active metabolite of amifostine(66). Amifostine has been documented as an intestinal radioprotector when administered to mice 30 min prior to radiation. These observations were made using the standard microcolony assay described earlier(102). This data makes WR-1065 an ideal candidate to test in our assay. Cells were plated at a density of 5,000 cells per well and allowed to grow for 5

days to generate spheroids. Cultures were incubated in the presence of either vehicle (PBS) or 2 mM WR-1065 for 2 h(103) and then exposed to increasing doses of ionizing radiation. Spheroids were immediately digested to single cells, replated at 5,000 cells per well embedded in a Matrigel dome, allowed to grow for 5 days, and then imaged.

Viable spheroids were quantified using Z-stack images spanning 1.5 mm in height and covering the entire Matrigel dome area (Fig. 14c). Images were manually stitched together (Fig. 14c) and a representative image of the matrigel dome is shown in Fig. 14d. Vehicle-treated (PBS) cultures exhibited reduced spheroid formation capacity with increasing doses of radiation, with very few spheroids visualized at the 8 Gy dose (Fig. 14e). WR-1065 afforded significant radioprotection, even at doses as high as 8 Gy (Fig. 14f). Thus, the SFA successfully replicated a colony formation assay in a 3D culture model.

Development of modified SFA that employs bioluminescence

To improve the throughput capabilities and quantitation of the assay, we engineered our stem cell-enriched epithelial spheroid line to stably express both Click Beetle Red Luciferase (CBR-Luc) and mCherry using lentiviral transduction (Fig. 15a)(84).

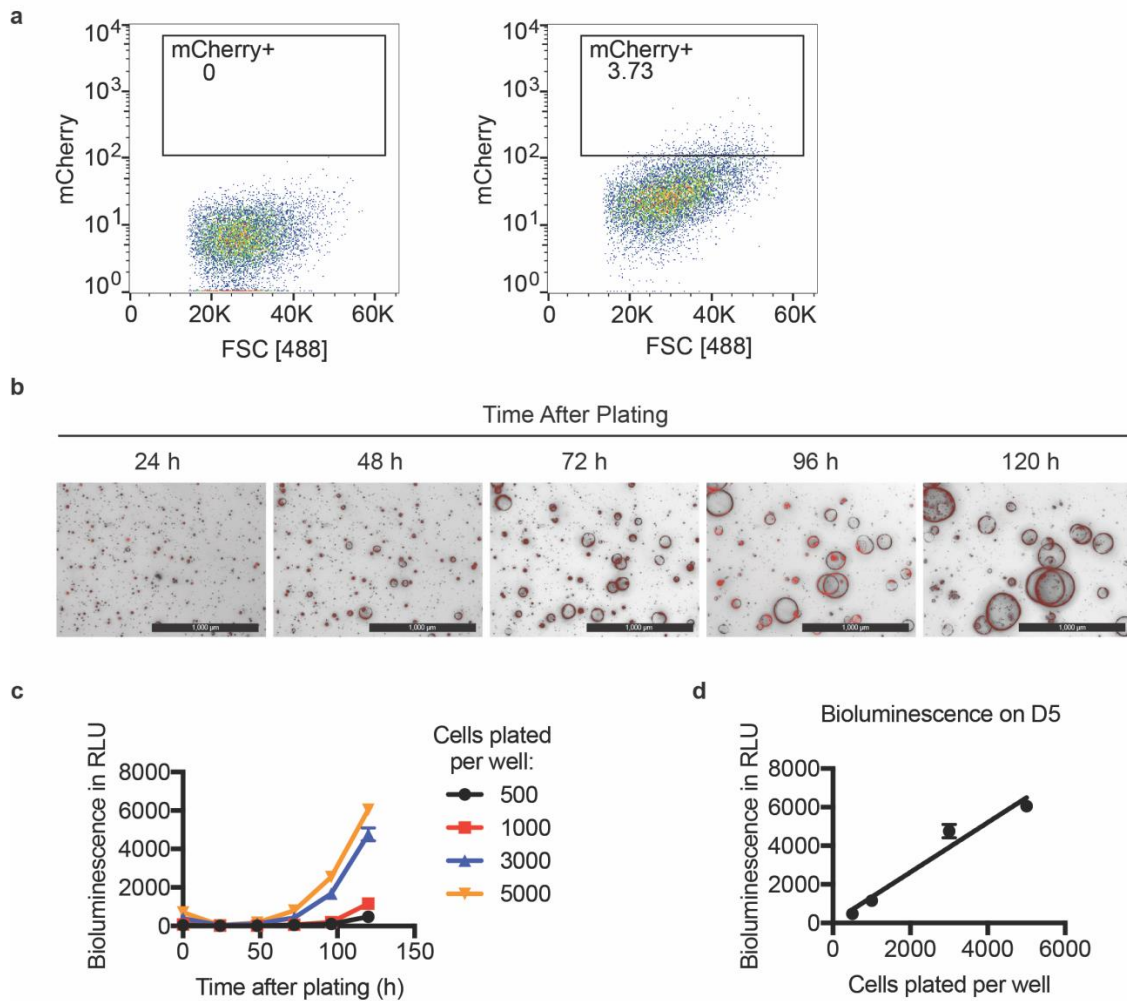


Figure 15 Generation of stem cell-enriched epithelial spheroid line stably expressing both Click Beetle Red Luciferase (CBR-Luc) and mCherry

Cells were transduced with FUW-CBR-luc-mCherry lentivirus and mCherry positive cells were isolated by flow cytometry (panel a). mCherry positive cells were plated and imaged at various times post plating. Representative bright field and mCherry (Texas Red) merged images are shown. Scale bars, 1000 μm (Panel b). Varying amounts of transduced cells were plated and bioluminescence was measured at the day of plating (day 0) and daily until day 5. Bioluminescence obtained for each sample was normalized to the bioluminescence measured in wells containing culture media and Matrigel but lacking cells (panel c). Cells plated per well at day 0 are plotted against the normalized bioluminescence measured per well on day 5 (panel d). $P < 0.05$ by Pearson correlation ($N=3$ per group). Error bars are \pm SEM.

In this way, mCherry expression could be used to select infected cells, while bioluminescence could be used to detect live cells as a function of time. Transduced cells were subjected to fluorescence-activated cell sorting (FACS) to isolate mCherry-positive cells (Fig. 15a), which were then plated at a density of 5,000 cells per well. As seen in Fig. 15b, transduced cells generated mCherry positive, stem cell-enriched epithelial spheroid cultures. Spheres were discernible as early as 48 h after plating a single cell suspension and were still viable 120 h after plating. Single cells were plated in triplicate at different densities and allowed to form spheroids for 5 days. Media containing D-luciferin was introduced into each well of the tissue culture plate and bioluminescence was measured in each well as a function of time: measurements were obtained at the time of plating (day 0) and daily from day 1 through 5 post plating. As shown in Fig. 15c, bioluminescence increased with time, indicating growth of cells. Bioluminescence measured on day 5 positively correlated with the number of cells plated in each well (Fig. 2d, $r=0.9772$, $R^2=0.955$) demonstrating that bioluminescence could be used to monitor the growth of cells in 3D spheroid cultures.

Bioluminescent SFA to assay radioprotection

The ability of the bioluminescent SFA to demonstrate WR-1065-mediated radioprotection in spheroid cultures was tested. Single cells were plated at a density of 5,000 cells per well and cultured for 5 days. Stem cell enriched-epithelial spheroid cultures were incubated in the presence of PBS (vehicle) or 2 mM WR-1065 for 2 h and were then either mock-irradiated or exposed to increasing doses of ionizing radiation. Spheroids were immediately dissociated to single cells, after which 3,000

cells were plated per well and cultured for 5 days. Representative images of day 5 spheroid cultures are shown in Fig. 16a and results from bioluminescence measurements (day 5) in Fig. 16b.

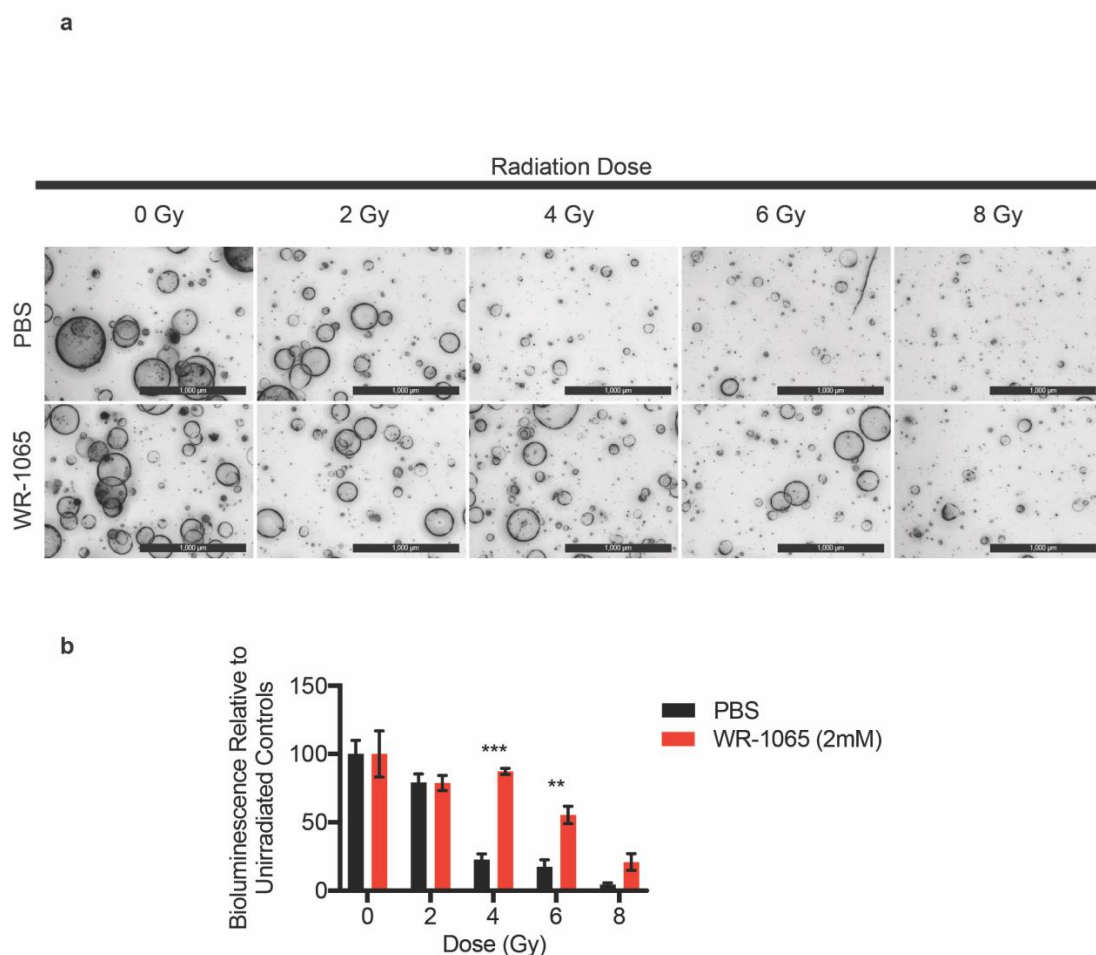


Figure 16 Spheroid Formation Assay for identifying radioprotectors *in vitro*

Stem cell-enriched epithelial spheroid cultures were incubated in the presence of vehicle or 2 mM WR-1065 for 2 h and then either mock irradiated or exposed to increasing doses of ionizing radiation. Spheroids were immediately dissociated to single cells and 3,000 cells were plated per well in triplicate and cultured for 5 days. Representative bright field images (panel a) (Scale bars, 1000 μ m) and corresponding bioluminescence measurements (panel b) are shown for day 5 samples. ** $P < 0.01$, *** $P < 0.001$ by two-tailed, Student's t test ($N = 3$ per group). Error bars are \pm SEM.

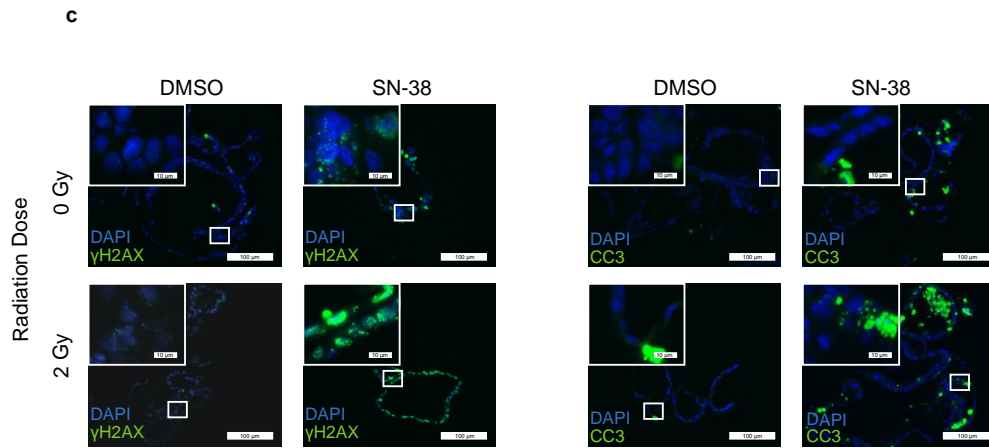
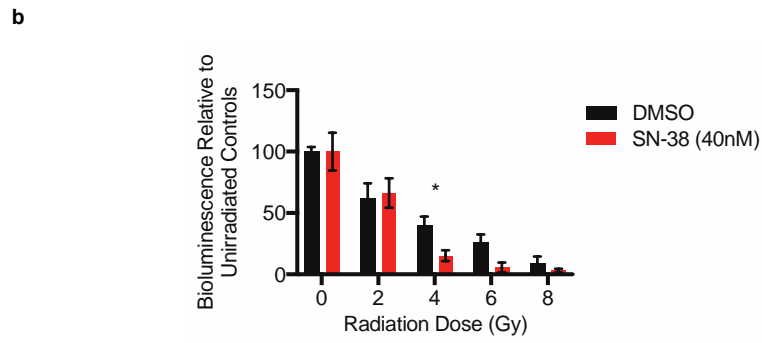
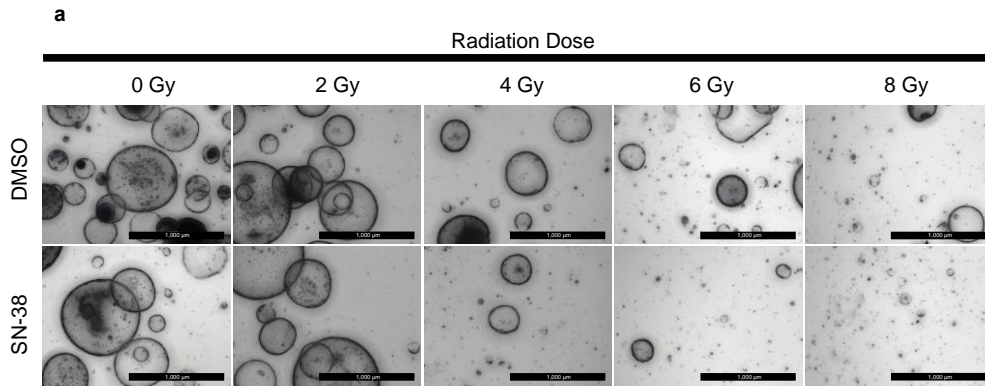
After normalizing bioluminescence measurements to that of non-irradiated controls, significantly increased relative bioluminescence was observed at 4 and 6 Gy doses. Taken together, these results demonstrated that WR-1065 provided radioprotection and validates the bioluminescent SFA for identifying novel radioprotectors.

Application of Bioluminescent SFA for identifying radiosensitizers

The SFA was also tested for its ability to detect radiosensitizers. Irinotecan, a topoisomerase I inhibitor used clinically to treat colorectal cancer(104), is known to radiosensitize cells and cause mucositis and diarrhea in both patients and mice. We tested the capacity of the SFA to correctly identify radiosensitizers by treating cells with SN-38, the active metabolite of irinotecan. Cells were plated at a density of 5,000 cells per well and allowed to grow for 5 days. Stem cell enriched-epithelial spheroid cultures were incubated in the presence of DMSO (vehicle) or 40 nM SN-38 for 24 h, and then either mock irradiated or exposed to increasing doses of ionizing radiation. Spheroids were then immediately dissociated to single cells and 3,000 cells were plated per well in triplicate and cultured for 8 days. As expected, fewer spheroids were visualized in SN-38 treated cultures relative to vehicle-treated cultures in a dose dependent manner (Fig. 17a).

Figure 17 Spheroid Formation Assay for identifying radiosensitizers *in vitro*.

Stem cell-enriched epithelial spheroid cultures were incubated in the presence of vehicle (DMSO) or 40 nM SN-38 for 24 h and then either mock irradiated or exposed to increasing doses of ionizing radiation. Spheroids were immediately dissociated to single cells and 3,000 cells were plated per well in triplicate and cultured for 5 days. Representative bright field images (panel a) (Scale bars, 1000 μm) and corresponding bioluminescence measurements (panel b) are shown for day 8 samples. * $P < 0.05$ by two-tailed, Student's t test (N=3 per group). Error bars are \pm SEM. Stem cell-enriched epithelial spheroid cultures were incubated in the presence of DMSO or 40 nM SN-38 for 24 h and then either mock irradiated or exposed to 2 Gy IR. Spheroids were harvested 3 h later and stained for γH2AX or cleaved caspase-3. Representative images are shown. Scale bars, 100 μm and 10 μm (inset) (Panel c).



Concordantly, significantly less relative bioluminescence was measured in SN-38 treated cultures relative to vehicle-treated cultures at 4 Gy of IR (Fig. 17b), demonstrating that irinotecan was functioning as a radiosensitizer in this assay.

Spheroids were also analyzed for the presence of DNA double strand breaks (DSBs) and apoptosis following SN-38 and IR treatments. Spheroid cultures were incubated in the presence of DMSO or 40 nM SN-38 for 24 h and then either mock irradiated or exposed to 2 Gy IR. The culture media was immediately replaced with fresh media lacking SN-38 and spheroids were cultured for an additional 3 h. Spheroids were then processed and stained for antibodies specific for either γ H2AX (gamma H2A histone family, member X) to assess DNA DSBs or for cleaved caspase 3 to assess apoptosis (Fig. 17c). SN-38 as a single agent induced more DNA DSBs and apoptotic cell death than did exposure to 2Gy IR alone. However, the combination of SN-38 and IR induced substantially more DNA DSBs and apoptosis than either agent alone, supporting a role for SN-38 as a radiosensitizer.

Discussion

The development of a rapid, high throughput assay that can be performed *in vitro* to identify novel GI radioprotectors and radiosensitizers has the potential to greatly impact the field of oncology. This is due to the fact that one of the major side effects of chemotherapy and radiation therapy is toxicity to the small intestine. The current gold standard Withers and Elkind assay is costly, low throughput, and time consuming(69), and currently impossible to do in human tissue, which has limited the discovery of novel modulators of radiation responses in normal tissue. Here we describe a novel *in vitro* assay for evaluating intestinal radioprotectors and radiosensitizers that overcomes these previous limitations. Our assay is rapid, high throughput, closely approximates more time-consuming methods, and could be easily extended to human tissues as needed.

Our assay employs three-dimensional (3D) cultures that are enriched for SI stem cells and grow as multicellular spheroids that may better approximate *in vivo* biology than standard 2D cultures (72). In addition, we have created intestinal stem cell lines with a luciferase reporter that acts as a surrogate for live spheroids after a cytotoxic insult since luciferase requires ATP for its enzymatic activity(105). This facile system will enable screens using unbiased small molecule libraries (106) or CRISPR/Cas9 systems(107) that could quickly identify targets that radiosensitize or radioprotect the intestine(105). Finally, although the SFA described herein employs stem cell-enriched epithelial spheroid cultures derived from the small intestine, it should be feasible with any normal or malignant tissues that grows as multicellular spheroids *ex vivo*(108).

Chapter 5: Discussion

In this study we showed that 24 h fasting promotes organismal survival after otherwise-lethal doses of abdominal radiation. Similar to previous work done in our lab where fasted mice were exposed to high dose etoposide, this host radioprotection was traced to the small intestine (71). Specifically, we showed that fasting increased SI stem cell survival and promoted intestinal epithelial recovery following radiation insult. This increased stem cell survival may be due, at least in part, to reduced early apoptosis evidenced in crypt cells.

Although we were able to show significant protection of the crypt base columnar Lgr5+ stem cells and modest protection of the Bmi1+ stem cells, we cannot rule out that other intestinal epithelial cells are playing a role in fasting-mediated intestinal radioprotection. In the introduction, it was briefly explained that small intestinal stem cells are thought to exist in two main groups; the crypt base columnar and the +4 cells. These distinct groups have been described to have discrete physiological roles in maintaining homeostasis and functioning as a reserve stem cell pool, respectively (65). As the small intestine is the second most radiosensitive organ in the body, it is not surprising that many research groups have evaluated the potential role of different stem cell populations in SI response to radiation injury (41). Cells at the +4 position from the crypt base are quiescent and therefore thought to have an increased capacity to withstand radiation injury than the rapid cycling CBCs (109). This notion is supported by studies that have shown that Lgr5+ CBCs cells decreased quickly after exposure to radiation (70). Proliferation and cell progeny arising from Bmi1, mTert and Lrig marked +4 stem cells after radiation injury has also been reported, supporting

their role as a reserve stem cell pool with regenerative capacities (59, 60, 110). This data is confounded by the fact that quiescent cell markers are co-expressed with Lgr5+ (61, 90) and that Lgr5+ cell depletion impairs intestinal regeneration after radiation injury (88). Moreover, it has been shown that a label retaining population of Lgr5+ stem cells is destined to differentiate into Paneth cells (90). This label-retaining population has the capacity to revert to a multipotent state after intestinal injury and co-expresses +4 stem cell markers previously reported to repopulate SI epithelium after radiation (90). It is thus plausible that the Lgr5+ population is composed of multiple subpopulations: the rapid cycling cells that maintain intestinal epithelial homeostasis and the quiescent cells that serve as injury-inducible reserve stem cells (90). Clearly, intestinal stem cell dynamics are complex and will need further studying to better understand the intricacies of this organ. The development of newer technologies, such as single cell sequencing (111) and imaging mass cytometry (112) will provide invaluable insights in understanding the shifts in SI stem cell populations that occur in homeostasis and pathologies.

In a highly proliferative environment such as the SI stem cell compartment, it is reasonable to hypothesize that dietary interventions would affect stem cell function, number and/or interactions with other niche cells. Prolonged fasting has been shown to increase intestinal stem cell (ISC) organoid-forming capacity (113). ISCs from 24 h fasted mice activated a fatty acid oxidation gene expression profile, that persists even when the crypts are grown in nutrient rich media for 48h and mediated the enhanced stemness afforded by fasting (113). Finally, the age dependent decline in ISC stem

cell number and function seen in mice is improved by fasting and fatty acid oxidation agonists. The energy metabolism shift from carbohydrate to ketone body-based that occurs during fasting may be contributing to the recuperation from radiation toxicity as fatty acid oxidation has been shown to increase stemness in the ISCs.

In regards to Lgr5+ cells, it has been shown that a prolonged fast of 48h does not change the number of Lgr5+ stem cells (113, 114) but upon re-feeding, Lgr5+ stem cells contribute 40% less towards SI repopulation when compared to non-fasted controls (114). Contrary to the reduced contribution of Lgr5+ cells upon re-feeding, a rare subpopulation of dormant stem cells marked by mTert were found to be primed for activation by re-feeding (114). This priming of mTert cells occurred through PTEN inactivation. Strikingly, these mTert cells have been shown to produce Lgr5+ stem cells and contribute in SI epithelial recovery from radiation (60). Specifically, a radiation-induced increase in reactive oxygen species leads to HIF1a transactivation of Wnt2b. Increased Wnt2b is required for mTert cell activation and subsequent regeneration of the intestine (115).

Taken together, these studies suggest that fasting can prime the ISC through exclusive but complementary mechanisms. After 24h fasting, Lgr5+ ISCs have enhanced stemness through fatty acid oxidation activation and lower proliferation upon re-feeding. This enables them to be better equipped to withstand radiation damage. At the same time, a separate radiation-resistant quiescent mTert population is not only activated by the radiation injury but also primed during fasting to respond to mTORC signaling induced by re-feeding and contribute to renewal as active stem cells. A mechanism that is again mediated through PTEN phosphorylation. Future

studies should evaluate if dietary interventions with ketogenic diets, which promote fatty acid oxidation, are sufficient to recapitulate fasting-mediated radioprotection. The role of mTert cells in fasting-mediated protection should also be further studied.

Other dietary interventions have been shown to affect ISCs. Increases in Lgr5+ stemness were also documented after exposure of mice to a high-fat diet. In this case, there is cell-autonomous enhanced self-renewal capabilities and decreased dependency on the Paneth cells niche (116). On the other hand, chronic caloric restriction shifts ISCs toward self-renewal and away from differentiation through autocrine signaling from reduced mTORC activity in Paneth cells. Increased stem cell function was evidenced by elevation in the number of Lgr5+ and Paneth cells, a reduction of differentiated enterocytes, enhanced capacity to form organoids, and higher crypt regeneration after injury (117). Despite this evidence, caloric restriction has not successfully recapitulated fasting-mediated chemoprotection (37), thus it is unlikely that Paneth cell induction of stemness is part of our observed phenotype.

Intestinal cell apoptosis occurring within 24h of radiation is mediated through p53 induction of PUMA (118, 119), whereas those cells that survive do so through subsequent p21 signaling which induces cell-cycle arrest and DNA damage repair (48, 51). PUMA-deficient mice have decreased apoptosis in the stem and progenitor cell compartments, increased crypt regeneration and concomitant increase in survival following high-dose radiation (120). In our model, we observed reduction in apoptosis at 24h post-radiation in fasted crypts when compared to fed, suggesting that fasting could be affecting PUMA mediated crypt cell death. Evaluating crypt cell death at

timepoints after 24h, when mitotic-catastrophe occurs once cells re-enter the cell cycle resulting in significant radiation-induced CBC cell loss, could also shed light on the mechanism by which SI crypt cells are protected (121).

Although we did not see reduced Ki67 staining when observing whole SI crypts, Lgr5+ stem cells have been shown do have reduced BrdU incorporation after a 24 hour fast (71) and reduced Ki67 staining after a 48h fast, (114) when compared to fed controls. This suggests that fasting may decrease crypt cell death by reducing crypt proliferation, increased DNA repair and prevention of mitotic-catastrophe.

While fasting did prevent the acute toxicities of radiation in the SI epithelium, it did not protect from long-term toxicities as observed by fibrosis present in the pancreas or the intestinal submucosa. Thus, fasting-mediated protection could be context dependent based on the cell type and microenvironment. For example, fasting has been shown to be protective against chemotherapy-induced hematopoietic suppression in both mice and humans (122). In mice, upon re-feeding, fasting was also shown to promote hematopoietic stem cell self-renewal and regeneration (122). Other types of dietary intervention such as chronic caloric restriction has been shown to affect stem cell function and differentiation in the intestinal (117), muscular (123), neural (124) and hematologic systems (125), whereas prolonged fasting itself has not been as extensively studied in other stem cell niches. It is thus prudent to evaluate the phenotypic changes that occur in other stem cell compartments upon fasting and/or refeeding.

Although we have focused on genotoxic injury to stem cells, fasting has also been shown to protect against ischemia reperfusion injury (IRI) (126). IRI can occur in surgical procedures, heart attacks or strokes when blood flow to a tissue is impaired preventing oxygen and nutrient delivery. This results in decreased oxidative phosphorylation and buildup of toxic metabolites, after which restoration of blood flow can bring pro-inflammatory mediators which may further exacerbate oxidative stress and damage to the tissue (127). In rats, a 16h fast was shown to protect re-perfused hearts (128), a 2-day-fast was shown to decrease neuronal loss during brain ischemia (129) and fasting of a donor animal increased success of liver transplantation (130). Further studies have traced fasting-mediated IRI protection to expression of antioxidant enzymes (131), increased response to pro-survival factors (132) and activation of autophagy (133-135). This protection from different stressors highlights the broad range of fasting-mediated changes that can promote organismal health, hindering the possibility that a single pharmacologic or dietary intervention other than water only fasting will be able to recapitulate these effects.

Recently, a fasting mimicking diet (FMD) was developed to reproduce fasting-mediated health benefits without incurring in the risks of a long-term water only fast (136). In mice, the diet consisted of two 4d periods of decreased consumption and ad libitum feeding in between. This low in calorie and protein intake diet induces similar changes to fasting with decreased IGF-1, increased IGFBP-1, increased ketone bodies and decreased glucose which return to baseline levels upon re-feeding (136). In humans the diet was designed to last 5 days every month providing 34-54% of the regular caloric intake (9-10% protein, 34-47% carbohydrate and 44-56% fat) in order

to achieve the desired changes in biomarkers as described above. Mice on this diet exhibited increased hepatic regeneration upon re-feeding, immune system and muscle regeneration and rejuvenation, decreased age-related bone mineral density decline, reduced tumor incidence, reduced inflammation, increased hematopoietic and mesenchymal stem and progenitor cells, improved learning and memory in old animals, neurogenesis in adult mice, and finally increased lifespan (136).

Subsequent studies using this FMD in mice suggest it could be useful in the setting of multiple sclerosis (MS), cancer immunotherapy, diabetes, and inflammatory bowel disease. MS is an autoimmune disease where T-cells cause demyelination and neurodegeneration in the CNS (137). In a mouse model of MS, the FMD diet promoted remyelination through oligodendrocyte regeneration and decreased further oligodendrocyte loss through dampening of autoimmunity via reduction of monocytes and T cells (137). In combination with chemotherapy, FMD was as effective as fasting in reducing tumor progression and was shown to decrease tumor HO-1 expression resulting in decreased regulatory T cell activation, cytotoxic T cell recruitment to the tumors and increased T-cell mediated cytotoxicity (137). In the pancreas, inhibition of PKA or mTOR during the FMD cycles, promoted expression of the progenitor marker Ngn3 upon refeeding, which led to β -cell generation and reversal of diabetic phenotypes in mice (138). In the most recent study using FMD, it was found to reverse the phenotype of a chronic dextran sodium sulfate (DSS)-induced colitis (139). FMD reversal of an IBD-associated phenotype seen in chronic DSS-colitis is mediated by reduced intestinal inflammation by way of reduced immune infiltration, enrichment of protective bacteria in the gut microbiome, and increased intestinal regeneration upon

re-feeding. Interestingly, comparing FMD to cycles of 48 h water-only fasting showed that although water only fasting promoted intestinal regeneration, it did not revert the DSS-induced phenotype or promote the increased abundance of protective gut microbiome as in FMD treated mice.

Through modulation of a wide-gamut of host factors, fasting and fasting mediated diets can promote recovery from tissue injury and rejuvenation of cells. Moving forward, the proposed fasting mimicking diet should be evaluated in a clinical setting not only as a possible mechanism to reduce cancer-therapy toxicities, but also as an intervention that may increase stem cell renewal and thus impact many age-related disease processes.

Bibliography

1. McDougald, D., L. Gong, S. Srinivasan, E. Hild, L. Thompson, K. Takayama, S. A. Rice, and S. Kjelleberg. 2002. Defences against oxidative stress during starvation in bacteria. *Antonie Van Leeuwenhoek* 81: 3-13.
2. Jenkins, D. E., J. E. Schultz, and A. Martin. 1988. Starvation-induced cross protection against heat or H₂O₂ challenge in *Escherichia coli*. *J Bacteriol* 170: 3910-3914.
3. Longo, V. D., L. M. Ellerby, D. E. Bredesen, J. S. Valentine, and E. B. Gralla. 1997. Human Bcl-2 reverses survival defects in yeast lacking superoxide dismutase and delays death of wild-type yeast. *J Cell Biol* 137: 1581-1588.
4. Wei, M., P. Fabrizio, J. Hu, H. Ge, C. Cheng, L. Li, and V. D. Longo. 2008. Life span extension by calorie restriction depends on Rim15 and transcription factors downstream of Ras/PKA, Tor, and Sch9. *PLoS Genet* 4: e13.
5. Weinkove, D., J. R. Halstead, D. Gems, and N. Divecha. 2006. Long-term starvation and ageing induce AGE-1/PI 3-kinase-dependent translocation of DAF-16/FOXO to the cytoplasm. *BMC Biol* 4: 1.
6. Honjoh, S., T. Yamamoto, M. Uno, and E. Nishida. 2009. Signalling through RHEB-1 mediates intermittent fasting-induced longevity in *C. elegans*. *Nature* 457: 726-730.
7. Lee, S. J., C. T. Murphy, and C. Kenyon. 2009. Glucose shortens the life span of *C. elegans* by downregulating DAF-16/FOXO activity and aquaporin gene expression. *Cell metabolism* 10: 379-391.

8. Fontana, L., L. Partridge, and V. D. Longo. 2010. Extending healthy life span--from yeast to humans. *Science* 328: 321-326.
9. Thevelein, J. M., and J. H. de Winder. 1999. Novel sensing mechanisms and targets for the cAMP-protein kinase A pathway in the yeast *Saccharomyces cerevisiae*. *Mol Microbiol* 33: 904-918.
10. Fabrizio, P., F. Pozza, S. D. Pletcher, C. M. Gendron, and V. D. Longo. 2001. Regulation of longevity and stress resistance by Sch9 in yeast. *Science* 292: 288-290.
11. Fabrizio, P., L. L. Liou, V. N. Moy, A. Diaspro, J. S. Valentine, E. B. Gralla, and V. D. Longo. 2003. SOD2 functions downstream of Sch9 to extend longevity in yeast. *Genetics* 163: 35-46.
12. Longo, V. D., and C. E. Finch. 2003. Evolutionary medicine: from dwarf model systems to healthy centenarians? *Science* 299: 1342-1346.
13. Johnson, T. E. 1990. Increased life-span of age-1 mutants in *Caenorhabditis elegans* and lower Gompertz rate of aging. *Science* 249: 908-912.
14. Paradis, S., M. Ailion, A. Toker, J. H. Thomas, and G. Ruvkun. 1999. A PDK1 homolog is necessary and sufficient to transduce AGE-1 PI3 kinase signals that regulate diapause in *Caenorhabditis elegans*. *Genes Dev* 13: 1438-1452.
15. Hsu, A. L., C. T. Murphy, and C. Kenyon. 2003. Regulation of aging and age-related disease by DAF-16 and heat-shock factor. *Science* 300: 1142-1145.
16. Henis-Korenblit, S., P. Zhang, M. Hansen, M. McCormick, S. J. Lee, M. Cary, and C. Kenyon. 2010. Insulin/IGF-1 signaling mutants reprogram ER stress

- response regulators to promote longevity. *Proc Natl Acad Sci U S A* 107: 9730-9735.
17. Larsen, P. L. 1993. Aging and resistance to oxidative damage in *Caenorhabditis elegans*. *Proc Natl Acad Sci U S A* 90: 8905-8909.
 18. Morris, J. Z., H. A. Tissenbaum, and G. Ruvkun. 1996. A phosphatidylinositol-3-OH kinase family member regulating longevity and diapause in *Caenorhabditis elegans*. *Nature* 382: 536-539.
 19. Tettweiler, G., M. Miron, M. Jenkins, N. Sonenberg, and P. F. Lasko. 2005. Starvation and oxidative stress resistance in *Drosophila* are mediated through the eIF4E-binding protein, d4E-BP. *Genes Dev* 19: 1840-1843.
 20. Vigne, P., M. Tauc, and C. Frelin. 2009. Strong dietary restrictions protect *Drosophila* against anoxia/reoxygenation injuries. *PLoS One* 4: e5422.
 21. Brown-Borg, H. M., and S. G. Rakoczy. 2000. Catalase expression in delayed and premature aging mouse models. *Experimental gerontology* 35: 199-212.
 22. Brown-Borg, H. M., S. G. Rakoczy, M. A. Romanick, and M. A. Kennedy. 2002. Effects of growth hormone and insulin-like growth factor-1 on hepatocyte antioxidative enzymes. *Exp Biol Med (Maywood)* 227: 94-104.
 23. Salmon, A. B., S. Murakami, A. Bartke, J. Kopchick, K. Yasumura, and R. A. Miller. 2005. Fibroblast cell lines from young adult mice of long-lived mutant strains are resistant to multiple forms of stress. *Am J Physiol Endocrinol Metab* 289: E23-29.
 24. Murakami, S. 2006. Stress resistance in long-lived mouse models. *Experimental gerontology* 41: 1014-1019.

25. Li, Y., W. Xu, M. W. McBurney, and V. D. Longo. 2008. SirT1 inhibition reduces IGF-I/IRS-2/Ras/ERK1/2 signaling and protects neurons. *Cell metabolism* 8: 38-48.
26. Lee, C., F. M. Safdie, L. Raffaghello, M. Wei, F. Madia, E. Parrella, D. Hwang, P. Cohen, G. Bianchi, and V. D. Longo. 2010. Reduced levels of IGF-I mediate differential protection of normal and cancer cells in response to fasting and improve chemotherapeutic index. *Cancer Res* 70: 1564-1572.
27. Tannenbaum, A. 1996. The dependence of tumor formation on the composition of the calorie-restricted diet as well as on the degree of restriction. 1945. *Nutrition* 12: 653-654.
28. Hursting, S. D., S. N. Perkins, and J. M. Phang. 1994. Calorie restriction delays spontaneous tumorigenesis in p53-knockout transgenic mice. *Proc Natl Acad Sci U S A* 91: 7036-7040.
29. Weindruch, R., and R. L. Walford. 1982. Dietary restriction in mice beginning at 1 year of age: effect on life-span and spontaneous cancer incidence. *Science* 215: 1415-1418.
30. Weindruch, R., R. L. Walford, S. Fligiel, and D. Guthrie. 1986. The retardation of aging in mice by dietary restriction: longevity, cancer, immunity and lifetime energy intake. *J Nutr* 116: 641-654.
31. Colman, R. J., R. M. Anderson, S. C. Johnson, E. K. Kastman, K. J. Kosmatka, T. M. Beasley, D. B. Allison, C. Cruzen, H. A. Simmons, J. W. Kemnitz, and R. Weindruch. 2009. Caloric restriction delays disease onset and mortality in rhesus monkeys. *Science* 325: 201-204.

32. Kalaany, N. Y., and D. M. Sabatini. 2009. Tumours with PI3K activation are resistant to dietary restriction. *Nature* 458: 725-731.
33. Descamps, O., J. Riondel, V. Ducros, and A. M. Roussel. 2005. Mitochondrial production of reactive oxygen species and incidence of age-associated lymphoma in OF1 mice: effect of alternate-day fasting. *Mech Ageing Dev* 126: 1185-1191.
34. Berrigan, D., S. N. Perkins, D. C. Haines, and S. D. Hursting. 2002. Adult-onset calorie restriction and fasting delay spontaneous tumorigenesis in p53-deficient mice. *Carcinogenesis* 23: 817-822.
35. Lee, C., L. Raffaghello, S. Brandhorst, F. M. Safdie, G. Bianchi, A. Martin-Montalvo, V. Pistoia, M. Wei, S. Hwang, A. Merlino, L. Emionite, R. de Cabo, and V. D. Longo. 2012. Fasting cycles retard growth of tumors and sensitize a range of cancer cell types to chemotherapy. *Science translational medicine* 4: 124ra127.
36. Bloechl-Daum, B., R. R. Deuson, P. Mavros, M. Hansen, and J. Herrstedt. 2006. Delayed nausea and vomiting continue to reduce patients' quality of life after highly and moderately emetogenic chemotherapy despite antiemetic treatment. *J Clin Oncol* 24: 4472-4478.
37. Brandhorst, S., M. Wei, S. Hwang, T. E. Morgan, and V. D. Longo. 2013. Short-term calorie and protein restriction provide partial protection from chemotoxicity but do not delay glioma progression. *Experimental gerontology* 48: 1120-1128.
38. Raffaghello, L., C. Lee, F. M. Safdie, M. Wei, F. Madia, G. Bianchi, and V. D. Longo. 2008. Starvation-dependent differential stress resistance protects

- normal but not cancer cells against high-dose chemotherapy. *Proc Natl Acad Sci U S A* 105: 8215-8220.
39. Safdie, F. M., T. Dorff, D. Quinn, L. Fontana, M. Wei, C. Lee, P. Cohen, and V. D. Longo. 2009. Fasting and cancer treatment in humans: A case series report. *Aging (Albany NY)* 1: 988-1007.
 40. Lee, J. E., J. I. Heo, S. H. Park, J. H. Kim, Y. J. Kho, H. J. Kang, H. Y. Chung, J. L. Yoon, and J. Y. Lee. 2011. Calorie restriction (CR) reduces age-dependent decline of non-homologous end joining (NHEJ) activity in rat tissues. *Experimental gerontology* 46: 891-896.
 41. Hall, E. J., and A. J. Giaccia. 2019. *Radiobiology for the radiologist*. Wolters Kluwer, Philadelphia.
 42. Potten, C. S., and M. Loeffler. 1990. Stem cells: attributes, cycles, spirals, pitfalls and uncertainties. Lessons for and from the crypt. *Development* 110: 1001-1020.
 43. Potten, C. S. 1990. A comprehensive study of the radiobiological response of the murine (BDF1) small intestine. *Int J Radiat Biol* 58: 925-973.
 44. Potten, C. S. 2001. Apoptosis in oral mucosa: lessons from the crypt. A commentary. *Oral Dis* 7: 81-85.
 45. Andreyev, H. J. 2007. Gastrointestinal problems after pelvic radiotherapy: the past, the present and the future. *Clin Oncol (R Coll Radiol)* 19: 790-799.
 46. Theis, V. S., R. Sripadam, V. Ramani, and S. Lal. 2010. Chronic radiation enteritis. *Clin Oncol (R Coll Radiol)* 22: 70-83.

47. Do, N. L., D. Nagle, and V. Y. Poylin. 2011. Radiation proctitis: current strategies in management. *Gastroenterol Res Pract* 2011: 917941.
48. Komarova, E. A., K. Christov, A. I. Faerman, and A. V. Gudkov. 2000. Different impact of p53 and p21 on the radiation response of mouse tissues. *Oncogene* 19: 3791-3798.
49. Merritt, A. J., C. S. Potten, C. J. Kemp, J. A. Hickman, A. Balmain, D. P. Lane, and P. A. Hall. 1994. The role of p53 in spontaneous and radiation-induced apoptosis in the gastrointestinal tract of normal and p53-deficient mice. *Cancer Res* 54: 614-617.
50. Merritt, A. J., T. D. Allen, C. S. Potten, and J. A. Hickman. 1997. Apoptosis in small intestinal epithelial from p53-null mice: evidence for a delayed, p53-independent G2/M-associated cell death after gamma-irradiation. *Oncogene* 14: 2759-2766.
51. Komarova, E. A., R. V. Kondratov, K. Wang, K. Christov, T. V. Golovkina, J. R. Goldblum, and A. V. Gudkov. 2004. Dual effect of p53 on radiation sensitivity in vivo: p53 promotes hematopoietic injury, but protects from gastro-intestinal syndrome in mice. *Oncogene* 23: 3265-3271.
52. Tinkum, K. L., L. S. White, L. Marpegan, E. Herzog, D. Piwnica-Worms, and H. Piwnica-Worms. 2013. Forkhead box O1 (FOXO1) protein, but not p53, contributes to robust induction of p21 expression in fasted mice. *J Biol Chem* 288: 27999-28008.
53. Umar, S. 2010. Intestinal stem cells. *Curr Gastroenterol Rep* 12: 340-348.

54. Creamer, B., R. G. Shorter, and J. Bamforth. 1961. The turnover and shedding of epithelial cells. I. The turnover in the gastro-intestinal tract. *Gut* 2: 110-118.
55. Cheng, H., and C. P. Leblond. 1974. Origin, differentiation and renewal of the four main epithelial cell types in the mouse small intestine. V. Unitarian Theory of the origin of the four epithelial cell types. *Am J Anat* 141: 537-561.
56. Bjerknes, M., and H. Cheng. 1999. Clonal analysis of mouse intestinal epithelial progenitors. *Gastroenterology* 116: 7-14.
57. Barker, N., J. H. van Es, J. Kuipers, P. Kujala, M. van den Born, M. Cozijnsen, A. Haegebarth, J. Korving, H. Begthel, P. J. Peters, and H. Clevers. 2007. Identification of stem cells in small intestine and colon by marker gene Lgr5. *Nature* 449: 1003-1007.
58. Potten, C. S., C. Booth, and D. M. Pritchard. 1997. The intestinal epithelial stem cell: the mucosal governor. *Int J Exp Pathol* 78: 219-243.
59. Tian, H., B. Biehs, S. Warming, K. G. Leong, L. Rangell, O. D. Klein, and F. J. de Sauvage. 2011. A reserve stem cell population in small intestine renders Lgr5-positive cells dispensable. *Nature* 478: 255-259.
60. Montgomery, R. K., D. L. Carlone, C. A. Richmond, L. Farilla, M. E. Kranendonk, D. E. Henderson, N. Y. Baffour-Awuah, D. M. Ambruzs, L. K. Fogli, S. Algra, and D. T. Breault. 2011. Mouse telomerase reverse transcriptase (mTert) expression marks slowly cycling intestinal stem cells. *Proc Natl Acad Sci U S A* 108: 179-184.
61. Munoz, J., D. E. Stange, A. G. Schepers, M. van de Wetering, B. K. Koo, S. Itzkovitz, R. Volckmann, K. S. Kung, J. Koster, S. Radulescu, K. Myant, R.

- Versteeg, O. J. Sansom, J. H. van Es, N. Barker, A. van Oudenaarden, S. Mohammed, A. J. Heck, and H. Clevers. 2012. The Lgr5 intestinal stem cell signature: robust expression of proposed quiescent '+4' cell markers. *EMBO J* 31: 3079-3091.
62. Jensen, K. B., C. A. Collins, E. Nascimento, D. W. Tan, M. Frye, S. Itami, and F. M. Watt. 2009. Lrig1 expression defines a distinct multipotent stem cell population in mammalian epidermis. *Cell Stem Cell* 4: 427-439.
63. Takeda, N., R. Jain, M. R. LeBoeuf, Q. Wang, M. M. Lu, and J. A. Epstein. 2011. Interconversion between intestinal stem cell populations in distinct niches. *Science* 334: 1420-1424.
64. Breault, D. T., I. M. Min, D. L. Carlone, L. G. Farilla, D. M. Ambruzs, D. E. Henderson, S. Algra, R. K. Montgomery, A. J. Wagers, and N. Hole. 2008. Generation of mTert-GFP mice as a model to identify and study tissue progenitor cells. *Proc Natl Acad Sci U S A* 105: 10420-10425.
65. Barker, N. 2014. Adult intestinal stem cells: critical drivers of epithelial homeostasis and regeneration. *Nature reviews. Molecular cell biology* 15: 19-33.
66. Kouvaris, J. R., V. E. Kouloulis, and L. J. Vlahos. 2007. Amifostine: the first selective-target and broad-spectrum radioprotector. *Oncologist* 12: 738-747.
67. Franken, N. A., H. M. Rodermond, J. Stap, J. Haveman, and C. van Bree. 2006. Clonogenic assay of cells in vitro. *Nat Protoc* 1: 2315-2319.

68. Hidalgo, I. J., T. J. Raub, and R. T. Borchardt. 1989. Characterization of the human colon carcinoma cell line (Caco-2) as a model system for intestinal epithelial permeability. *Gastroenterology* 96: 736-749.
69. Withers, H. R., and M. M. Elkind. 1970. Microcolony survival assay for cells of mouse intestinal mucosa exposed to radiation. *Int J Radiat Biol Relat Stud Phys Chem Med* 17: 261-267.
70. Yan, K. S., L. A. Chia, X. Li, A. Ootani, J. Su, J. Y. Lee, N. Su, Y. Luo, S. C. Heilshorn, M. R. Amieva, E. Sangiorgi, M. R. Capecchi, and C. J. Kuo. 2012. The intestinal stem cell markers Bmi1 and Lgr5 identify two functionally distinct populations. *Proc Natl Acad Sci U S A* 109: 466-471.
71. Tinkum, K. L., K. M. Stemler, L. S. White, A. J. Loza, S. Jeter-Jones, B. M. Michalski, C. Kuzmicki, R. Pless, T. S. Stappenbeck, D. Piwnica-Worms, and H. Piwnica-Worms. 2015. Fasting protects mice from lethal DNA damage by promoting small intestinal epithelial stem cell survival. *Proc Natl Acad Sci U S A* 112: E7148-7154.
72. Miyoshi, H., and T. S. Stappenbeck. 2013. In vitro expansion and genetic modification of gastrointestinal stem cells in spheroid culture. *Nat Protoc* 8: 2471-2482.
73. Siegel, R., J. Ma, Z. Zou, and A. Jemal. 2014. Cancer statistics, 2014. *CA Cancer J Clin* 64: 9-29.
74. Von Hoff, D. D., R. K. Ramanathan, M. J. Borad, D. A. Laheru, L. S. Smith, T. E. Wood, R. L. Korn, N. Desai, V. Trieu, J. L. Iglesias, H. Zhang, P. Soon-Shiong, T. Shi, N. V. Rajeshkumar, A. Maitra, and M. Hidalgo. 2011.

- Gemcitabine plus nab-paclitaxel is an active regimen in patients with advanced pancreatic cancer: a phase I/II trial. *J Clin Oncol* 29: 4548-4554.
75. Macia, I. G. M., A. Lucas Calduch, and E. C. Lopez. 2011. Radiobiology of the acute radiation syndrome. *Rep Pract Oncol Radiother* 16: 123-130.
76. Kelly, P., P. Das, C. C. Pinnix, S. Beddar, T. Briere, M. Pham, S. Krishnan, M. E. Delclos, and C. H. Crane. 2013. Duodenal toxicity after fractionated chemoradiation for unresectable pancreatic cancer. *International journal of radiation oncology, biology, physics* 85: e143-149.
77. Ribeiro, R. A., C. W. Wanderley, D. V. Wong, J. M. Mota, C. A. Leite, M. H. Souza, F. Q. Cunha, and R. C. Lima-Junior. 2016. Irinotecan- and 5-fluorouracil-induced intestinal mucositis: insights into pathogenesis and therapeutic perspectives. *Cancer Chemother Pharmacol* 78: 881-893.
78. Hapani, S., D. Chu, and S. Wu. 2009. Risk of gastrointestinal perforation in patients with cancer treated with bevacizumab: a meta-analysis. *The lancet oncology* 10: 559-568.
79. Ben-Josef, E., M. Schipper, I. R. Francis, S. Hadley, R. Ten-Haken, T. Lawrence, D. Normolle, D. M. Simeone, C. Sonnenday, R. Abrams, W. Leslie, G. Khan, and M. M. Zalupski. 2012. A phase I/II trial of intensity modulated radiation (IMRT) dose escalation with concurrent fixed-dose rate gemcitabine (FDR-G) in patients with unresectable pancreatic cancer. *International journal of radiation oncology, biology, physics* 84: 1166-1171.

80. Hatzivassiliou, G., F. Zhao, D. E. Bauer, C. Andreadis, A. N. Shaw, D. Dhanak, S. R. Hingorani, D. A. Tuveson, and C. B. Thompson. 2005. ATP citrate lyase inhibition can suppress tumor cell growth. *Cancer Cell* 8: 311-321.
81. Fujimoto, T. N., L. E. Colbert, Y. Huang, J. M. Molkenline, A. Deorukhkar, L. Baseler, M. C. Bonilla, M. Yu, D. Lin, S. Gupta, P. K. Cabeceiras, C. V. Kingsley, R. C. Tailor, G. O. Sawakuchi, E. J. Koay, H. Piwnica-Worms, A. Maitra, and C. M. Taniguchi. 2019. Selective EGLN Inhibition Enables Ablative Radiotherapy and Improves Survival in Unresectable Pancreatic Cancer. *Cancer Res* 79: 2327-2338.
82. Molkenline, J. M., T. N. Fujimoto, T. D. Horvath, A. J. Grossberg, C. J. G. Garcia, A. Deorukhkar, M. de la Cruz Bonilla, D. Lin, E. L. G. Samuel, W. K. Chan, P. L. Lorenzi, H. Piwnica-Worms, R. Dantzer, J. M. Tour, K. A. Mason, and C. M. Taniguchi. 2019. Enteral Activation of WR-2721 Mediates Radioprotection and Improved Survival from Lethal Fractionated Radiation. *Scientific reports* 9: 1949.
83. Stack, E. C., C. Wang, K. A. Roman, and C. C. Hoyt. 2014. Multiplexed immunohistochemistry, imaging, and quantitation: a review, with an assessment of Tyramide signal amplification, multispectral imaging and multiplex analysis. *Methods* 70: 46-58.
84. Powell, E., J. Shao, Y. Yuan, H.-C. Chen, S. Cai, G. V. Echeverria, N. Mistry, K. F. Decker, C. Schlosberg, K.-A. Do, J. R. Edwards, H. Liang, D. Piwnica-Worms, and H. Piwnica-Worms. 2016. p53 deficiency linked to B cell translocation gene 2 (BTG2) loss enhances metastatic potential by promoting

- tumor growth in primary and metastatic sites in patient-derived xenograft (PDX) models of triple-negative breast cancer. *Breast Cancer Research : BCR* 18: 13.
85. Safdie, F., S. Brandhorst, M. Wei, W. Wang, C. Lee, S. Hwang, P. S. Conti, T. C. Chen, and V. D. Longo. 2012. Fasting enhances the response of glioma to chemo- and radiotherapy. *PLoS One* 7: e44603.
 86. Klement, R. J., and C. E. Champ. 2014. Calories, carbohydrates, and cancer therapy with radiation: exploiting the five R's through dietary manipulation. *Cancer metastasis reviews* 33: 217-229.
 87. Hingorani, S. R., L. Wang, A. S. Multani, C. Combs, T. B. Deramandt, R. H. Hruban, A. K. Rustgi, S. Chang, and D. A. Tuveson. 2005. Trp53R172H and KrasG12D cooperate to promote chromosomal instability and widely metastatic pancreatic ductal adenocarcinoma in mice. *Cancer Cell* 7: 469-483.
 88. Metcalfe, C., N. M. Kljavin, R. Ybarra, and F. J. de Sauvage. 2014. Lgr5+ stem cells are indispensable for radiation-induced intestinal regeneration. *Cell Stem Cell* 14: 149-159.
 89. van Es, J. H., T. Sato, M. van de Wetering, A. Lyubimova, A. N. Yee Nee, A. Gregorieff, N. Sasaki, L. Zeinstra, M. van den Born, J. Korving, A. C. M. Martens, N. Barker, A. van Oudenaarden, and H. Clevers. 2012. Dll1+ secretory progenitor cells revert to stem cells upon crypt damage. *Nat Cell Biol* 14: 1099-1104.
 90. Buczacki, S. J., H. I. Zecchini, A. M. Nicholson, R. Russell, L. Vermeulen, R. Kemp, and D. J. Winton. 2013. Intestinal label-retaining cells are secretory precursors expressing Lgr5. *Nature* 495: 65-69.

91. Tetteh, P. W., O. Basak, H. F. Farin, K. Wiebrands, K. Kretzschmar, H. Begthel, M. van den Born, J. Korving, F. de Sauvage, J. H. van Es, A. van Oudenaarden, and H. Clevers. 2016. Replacement of Lost Lgr5-Positive Stem Cells through Plasticity of Their Enterocyte-Lineage Daughters. *Cell Stem Cell* 18: 203-213.
92. Asfaha, S., Y. Hayakawa, A. Muley, S. Stokes, T. A. Graham, R. E. Ericksen, C. B. Westphalen, J. von Burstin, T. L. Mastracci, D. L. Worthley, C. Guha, M. Quante, A. K. Rustgi, and T. C. Wang. 2015. Krt19(+)/Lgr5(-) Cells Are Radioresistant Cancer-Initiating Stem Cells in the Colon and Intestine. *Cell Stem Cell* 16: 627-638.
93. Yan, K. S., O. Gevaert, G. X. Y. Zheng, B. Anchang, C. S. Probert, K. A. Larkin, P. S. Davies, Z. F. Cheng, J. S. Kaddis, A. Han, K. Roelf, R. I. Calderon, E. Cynn, X. Hu, K. Mandleywala, J. Wilhelmy, S. M. Grimes, D. C. Corney, S. C. Boutet, J. M. Terry, P. Belgrader, S. B. Ziraldo, T. S. Mikkelsen, F. Wang, R. J. von Furstenberg, N. R. Smith, P. Chandrakesan, R. May, M. A. S. Chrissy, R. Jain, C. A. Cartwright, J. C. Niland, Y. K. Hong, J. Carrington, D. T. Breault, J. Epstein, C. W. Houchen, J. P. Lynch, M. G. Martin, S. K. Plevritis, C. Curtis, H. P. Ji, L. Li, S. J. Henning, M. H. Wong, and C. J. Kuo. 2017. Intestinal Enteroendocrine Lineage Cells Possess Homeostatic and Injury-Inducible Stem Cell Activity. *Cell Stem Cell* 21: 78-90 e76.
94. Yu, S., K. Tong, Y. Zhao, I. Balasubramanian, G. S. Yap, R. P. Ferraris, E. M. Bonder, M. P. Verzi, and N. Gao. 2018. Paneth Cell Multipotency Induced by Notch Activation following Injury. *Cell Stem Cell* 23: 46-59 e45.

95. Schmitt, M., M. Schewe, A. Sacchetti, D. Feijtel, W. S. van de Geer, M. Teeuwssen, H. F. Sleddens, R. Joosten, M. E. van Royen, H. J. G. van de Werken, J. van Es, H. Clevers, and R. Fodde. 2018. Paneth Cells Respond to Inflammation and Contribute to Tissue Regeneration by Acquiring Stem-like Features through SCF/c-Kit Signaling. *Cell reports* 24: 2312-2328 e2317.
96. Ayyaz, A., S. Kumar, B. Sangiorgi, B. Ghoshal, J. Gosio, S. Ouladan, M. Fink, S. Barutcu, D. Trcka, J. Shen, K. Chan, J. L. Wrana, and A. Gregorieff. 2019. Single-cell transcriptomes of the regenerating intestine reveal a revival stem cell. *Nature*.
97. de Groot, S., M. P. Vreeswijk, M. J. Welters, G. Gravesteijn, J. J. Boei, A. Jochems, D. Houtsma, H. Putter, J. J. van der Hoeven, J. W. Nortier, H. Pijl, and J. R. Kroep. 2015. The effects of short-term fasting on tolerance to (neo) adjuvant chemotherapy in HER2-negative breast cancer patients: a randomized pilot study. *BMC Cancer* 15: 652.
98. Dorff, T. B., S. Groshen, A. Garcia, M. Shah, D. Tsao-Wei, H. Pham, C. W. Cheng, S. Brandhorst, P. Cohen, M. Wei, V. Longo, and D. I. Quinn. 2016. Safety and feasibility of fasting in combination with platinum-based chemotherapy. *BMC Cancer* 16: 360.
99. Colbert, L. E., N. Rebuena, S. Moningi, S. Beddar, G. O. Sawakuchi, J. M. Herman, A. C. Koong, P. Das, E. B. Holliday, E. J. Koay, and C. M. Taniguchi. 2018. Dose escalation for locally advanced pancreatic cancer: How high can we go? *Adv Radiat Oncol* 3: 693-700.

100. Heydari, A. R., A. Unnikrishnan, L. V. Lucente, and A. Richardson. 2007. Caloric restriction and genomic stability. *Nucleic Acids Res* 35: 7485-7496.
101. Um, J. H., S. J. Kim, D. W. Kim, M. Y. Ha, J. H. Jang, D. W. Kim, B. S. Chung, C. D. Kang, and S. H. Kim. 2003. Tissue-specific changes of DNA repair protein Ku and mtHSP70 in aging rats and their retardation by caloric restriction. *Mech Ageing Dev* 124: 967-975.
102. Phan, D., X. Sui, D. T. Chen, S. M. Najjar, G. Jenster, and S. H. Lin. 2001. Androgen regulation of the cell-cell adhesion molecule-1 (Ceacam1) gene. *Molecular and cellular endocrinology* 184: 115-123.
103. Rubin, D. B., E. A. Drab, H. J. Kang, F. E. Baumann, and E. R. Blazek. 1996. WR-1065 and radioprotection of vascular endothelial cells. I. Cell proliferation, DNA synthesis and damage. *Radiat Res* 145: 210-216.
104. Fuchs, C., E. P. Mitchell, and P. M. Hoff. 2006. Irinotecan in the treatment of colorectal cancer. *Cancer Treat Rev* 32: 491-503.
105. Nakatsu, T., S. Ichiyama, J. Hiratake, A. Saldanha, N. Kobashi, K. Sakata, and H. Kato. 2006. Structural basis for the spectral difference in luciferase bioluminescence. *Nature* 440: 372-376.
106. Kim, K., R. Damoiseaux, A. J. Norris, L. Rivina, K. Bradley, M. E. Jung, R. A. Gatti, R. H. Schiestl, and W. H. McBride. 2011. High throughput screening of small molecule libraries for modifiers of radiation responses. *Int J Radiat Biol* 87: 839-845.

107. Cong, L., F. A. Ran, D. Cox, S. Lin, R. Barretto, N. Habib, P. D. Hsu, X. Wu, W. Jiang, L. A. Marraffini, and F. Zhang. 2013. Multiplex genome engineering using CRISPR/Cas systems. *Science* 339: 819-823.
108. Clevers, H. 2016. Modeling Development and Disease with Organoids. *Cell* 165: 1586-1597.
109. Pajonk, F., and E. Vlashi. 2013. Characterization of the stem cell niche and its importance in radiobiological response. *Semin Radiat Oncol* 23: 237-241.
110. Powell, A. E., Y. Wang, Y. Li, E. J. Poulin, A. L. Means, M. K. Washington, J. N. Higginbotham, A. Juchheim, N. Prasad, S. E. Levy, Y. Guo, Y. Shyr, B. J. Aronow, K. M. Haigis, J. L. Franklin, and R. J. Coffey. 2012. The pan-ErbB negative regulator Lrig1 is an intestinal stem cell marker that functions as a tumor suppressor. *Cell* 149: 146-158.
111. Wen, L., and F. Tang. 2016. Single-cell sequencing in stem cell biology. *Genome Biol* 17: 71.
112. Chang, Q., O. I. Ornatsky, I. Siddiqui, A. Loboda, V. I. Baranov, and D. W. Hedley. 2017. Imaging Mass Cytometry. *Cytometry. Part A : the journal of the International Society for Analytical Cytology* 91: 160-169.
113. Mihaylova, M. M., C. W. Cheng, A. Q. Cao, S. Tripathi, M. D. Mana, K. E. Bauer-Rowe, M. Abu-Remaileh, L. Clavain, A. Erdemir, C. A. Lewis, E. Freinkman, A. S. Dickey, A. R. La Spada, Y. Huang, G. W. Bell, V. Deshpande, P. Carmeliet, P. Katajisto, D. M. Sabatini, and O. H. Yilmaz. 2018. Fasting Activates Fatty Acid Oxidation to Enhance Intestinal Stem Cell Function during Homeostasis and Aging. *Cell Stem Cell* 22: 769-778 e764.

114. Richmond, C. A., M. S. Shah, L. T. Deary, D. C. Trotier, H. Thomas, D. M. Ambruzs, L. Jiang, B. B. Whiles, H. D. Rickner, R. K. Montgomery, A. Tovaglieri, D. L. Carlone, and D. T. Breault. 2015. Dormant Intestinal Stem Cells Are Regulated by PTEN and Nutritional Status. *Cell reports* 13: 2403-2411.
115. Suh, H. N., M. J. Kim, Y. S. Jung, E. M. Lien, S. Jun, and J. I. Park. 2017. Quiescence Exit of Tert(+) Stem Cells by Wnt/beta-Catenin Is Indispensable for Intestinal Regeneration. *Cell reports* 21: 2571-2584.
116. Beyaz, S., M. D. Mana, J. Roper, D. Kedrin, A. Saadatpour, S. J. Hong, K. E. Bauer-Rowe, M. E. Xifaras, A. Akkad, E. Arias, L. Pinello, Y. Katz, S. Shinagare, M. Abu-Remaileh, M. M. Mihaylova, D. W. Lamming, R. Dogum, G. Guo, G. W. Bell, M. Selig, G. P. Nielsen, N. Gupta, C. R. Ferrone, V. Deshpande, G. C. Yuan, S. H. Orkin, D. M. Sabatini, and O. H. Yilmaz. 2016. High-fat diet enhances stemness and tumorigenicity of intestinal progenitors. *Nature* 531: 53-58.
117. Yilmaz, Ö. H., P. Katajisto, D. W. Lamming, Y. Gültekin, K. E. Bauer-Rowe, S. Sengupta, K. Birsoy, A. Dursun, V. O. Yilmaz, and M. Selig. 2012. mTORC1 in the Paneth cell niche couples intestinal stem-cell function to calorie intake. *Nature* 486: 490.
118. Leibowitz, B. J., W. Qiu, H. Liu, T. Cheng, L. Zhang, and J. Yu. 2011. Uncoupling p53 functions in radiation-induced intestinal damage via PUMA and p21. *Mol Cancer Res* 9: 616-625.

119. Leibowitz, B. J., L. Wei, L. Zhang, X. Ping, M. Epperly, J. Greenberger, T. Cheng, and J. Yu. 2014. Ionizing irradiation induces acute haematopoietic syndrome and gastrointestinal syndrome independently in mice. *Nature communications* 5: 3494.
120. Qiu, W., E. B. Carson-Walter, H. Liu, M. Epperly, J. S. Greenberger, G. P. Zambetti, L. Zhang, and J. Yu. 2008. PUMA regulates intestinal progenitor cell radiosensitivity and gastrointestinal syndrome. *Cell Stem Cell* 2: 576-583.
121. Hua, G., T. H. Thin, R. Feldman, A. Haimovitz-Friedman, H. Clevers, Z. Fuks, and R. Kolesnick. 2012. Crypt base columnar stem cells in small intestines of mice are radioresistant. *Gastroenterology* 143: 1266-1276.
122. Cheng, C. W., G. B. Adams, L. Perin, M. Wei, X. Zhou, B. S. Lam, S. Da Sacco, M. Mirisola, D. I. Quinn, T. B. Dorff, J. J. Kopchick, and V. D. Longo. 2014. Prolonged fasting reduces IGF-1/PKA to promote hematopoietic-stem-cell-based regeneration and reverse immunosuppression. *Cell Stem Cell* 14: 810-823.
123. Cerletti, M., Y. C. Jang, L. W. Finley, M. C. Haigis, and A. J. Wagers. 2012. Short-term calorie restriction enhances skeletal muscle stem cell function. *Cell Stem Cell* 10: 515-519.
124. Lee, J., W. Duan, J. M. Long, D. K. Ingram, and M. P. Mattson. 2000. Dietary restriction increases the number of newly generated neural cells, and induces BDNF expression, in the dentate gyrus of rats. *J Mol Neurosci* 15: 99-108.
125. Tang, D., S. Tao, Z. Chen, I. O. Koliesnik, P. G. Calmes, V. Hoerr, B. Han, N. Gebert, M. Zornig, B. Loffler, Y. Morita, and K. L. Rudolph. 2016. Dietary

- restriction improves repopulation but impairs lymphoid differentiation capacity of hematopoietic stem cells in early aging. *J Exp Med* 213: 535-553.
126. Brandhorst, S., E. Harputlugil, J. R. Mitchell, and V. D. Longo. 2017. Protective effects of short-term dietary restriction in surgical stress and chemotherapy. *Ageing research reviews* 39: 68-77.
127. Wu, M. Y., G. T. Yiang, W. T. Liao, A. P. Tsai, Y. L. Cheng, P. W. Cheng, C. Y. Li, and C. J. Li. 2018. Current Mechanistic Concepts in Ischemia and Reperfusion Injury. *Cell Physiol Biochem* 46: 1650-1667.
128. Schneider, C. A., and H. Taegtmeyer. 1991. Fasting in vivo delays myocardial cell damage after brief periods of ischemia in the isolated working rat heart. *Circulation research* 68: 1045-1050.
129. Marie, C., A. M. Bralet, S. Gueldry, and J. Bralet. 1990. Fasting prior to transient cerebral ischemia reduces delayed neuronal necrosis. *Metab Brain Dis* 5: 65-75.
130. Sumimoto, R., J. H. Southard, and F. O. Belzer. 1993. Livers from fasted rats acquire resistance to warm and cold ischemia injury. *Transplantation* 55: 728-732.
131. Verweij, M., M. van de Ven, J. R. Mitchell, S. van den Engel, J. H. Hoeijmakers, J. N. Ijzermans, and R. W. de Bruin. 2011. Glucose supplementation does not interfere with fasting-induced protection against renal ischemia/reperfusion injury in mice. *Transplantation* 92: 752-758.
132. Mitchell, J. R., M. Verweij, K. Brand, M. van de Ven, N. Goemaere, S. van den Engel, T. Chu, F. Forrer, C. Muller, M. de Jong, I. W. van, I. J. JN, J. H.

- Hoeijmakers, and R. W. de Bruin. 2010. Short-term dietary restriction and fasting precondition against ischemia reperfusion injury in mice. *Aging Cell* 9: 40-53.
133. Godar, R. J., X. Ma, H. Liu, J. T. Murphy, C. J. Weinheimer, A. Kovacs, S. D. Crosby, P. Saftig, and A. Diwan. 2015. Repetitive stimulation of autophagy-lysosome machinery by intermittent fasting preconditions the myocardium to ischemia-reperfusion injury. *Autophagy* 11: 1537-1560.
134. Jiang, M., K. Liu, J. Luo, and Z. Dong. 2010. Autophagy is a renoprotective mechanism during in vitro hypoxia and in vivo ischemia-reperfusion injury. *Am J Pathol* 176: 1181-1192.
135. Papadakis, M., G. Hadley, M. Xilouri, L. C. Hoyte, S. Nagel, M. M. McMenamin, G. Tsaknakis, S. M. Watt, C. W. Drakesmith, R. Chen, M. J. Wood, Z. Zhao, B. Kessler, K. Vekrellis, and A. M. Buchan. 2013. Tsc1 (hamartin) confers neuroprotection against ischemia by inducing autophagy. *Nature medicine* 19: 351-357.
136. Brandhorst, S., I. Y. Choi, M. Wei, C. W. Cheng, S. Sedrakyan, G. Navarrete, L. Dubeau, L. P. Yap, R. Park, M. Vinciguerra, S. Di Biase, H. Mirzaei, M. G. Mirisola, P. Childress, L. Ji, S. Groshen, F. Penna, P. Odetti, L. Perin, P. S. Conti, Y. Ikeno, B. K. Kennedy, P. Cohen, T. E. Morgan, T. B. Dorff, and V. D. Longo. 2015. A Periodic Diet that Mimics Fasting Promotes Multi-System Regeneration, Enhanced Cognitive Performance, and Healthspan. *Cell metabolism* 22: 86-99.

137. Choi, I. Y., L. Piccio, P. Childress, B. Bollman, A. Ghosh, S. Brandhorst, J. Suarez, A. Michalsen, A. H. Cross, T. E. Morgan, M. Wei, F. Paul, M. Bock, and V. D. Longo. 2016. A Diet Mimicking Fasting Promotes Regeneration and Reduces Autoimmunity and Multiple Sclerosis Symptoms. *Cell reports* 15: 2136-2146.
138. Cheng, C. W., V. Villani, R. Buono, M. Wei, S. Kumar, O. H. Yilmaz, P. Cohen, J. B. Sneddon, L. Perin, and V. D. Longo. 2017. Fasting-Mimicking Diet Promotes Ngn3-Driven beta-Cell Regeneration to Reverse Diabetes. *Cell* 168: 775-788 e712.
139. Rangan, P., I. Choi, M. Wei, G. Navarrete, E. Guen, S. Brandhorst, N. Enyati, G. Pasia, D. Maesincee, V. Ocon, M. Abdulridha, and V. D. Longo. 2019. Fasting-Mimicking Diet Modulates Microbiota and Promotes Intestinal Regeneration to Reduce Inflammatory Bowel Disease Pathology. *Cell reports* 26: 2704-2719 e2706.

Vita

Marimar de la Cruz Bonilla was born in San Juan, Puerto Rico, the daughter of Julia Bonilla Camacho and Francisco de la Cruz Cruz. After completing her work at the Residential Center of Educational Opportunities of Mayagüez (CROEM by its acronym in Spanish), Mayagüez, Puerto Rico in 2007, she entered the University of Puerto Rico in Mayagüez, Puerto Rico. She received the degree of Bachelor of Science with a major in biology from the University of Puerto Rico in May, 2011. In August of 2011 she entered into an MD/PhD program through a U54 Partnership for Excellence in Cancer Research grant between the University of Puerto Rico School of Medicine and The University of Texas MD Anderson Cancer Center UTHealth Graduate School of Biomedical Sciences.